AP42 Section:	9.2.1
Background Ch	2
Reference:	12
Title:	D. H. Lenschow and B. B. Hicks (eds.), *Global Tropospheric Chemistry*, National Center for Atmospheric Research, Boulder, CO, May 1989.

Global Tropospheric Chemistry

CHEMICAL FLUXES IN THE GLOBAL ATMOSPHERE

Report of the Workshop on Measurements of
Surface Exchange and Flux Divergence of
Chemical Species in the Global Atmosphere

Prepared by the
National Center for Atmospheric Research
P.O. Box 3000, Boulder, Colorado 80307

for

the National Science Foundation,
the National Aeronautics and Space Administration,
and the National Oceanic and Atmospheric Administration

Edited by
Donald H. Lenschow and Bruce B. Hicks

May 1989

1 KEY ASPECTS OF SPECIES RELATED TO GLOBAL BIOGEOCHEMICAL CYCLES

M. Andreae, A. C. Delany, S. Liu, J. Logan, L. P. Steele, H. Westberg, and R. Zika

The important roles played by various trace species in global biogeochemical cycles have been discussed in *Global Tropospheric Chemistry: Plans for the U.S. Research Effort* (UCAR, 1986). In this chapter, we will limit discussion to the surface exchange and flux divergence of the key trace species, and related research needs. The species included are classified into three major groups—the oxidant and odd nitrogen group, the sulfur group, and the carbon group. Critical studies for each group will be identified and discussed. We note, however, that many of the studies are related to each other; therefore, carrying out concurrent studies addressing several species at the same time offers considerable attraction.

The surface exchange rate of a chemical species is usually a function of surface properties such as the kind and condition of vegetation, nutrient level, temperature, and moisture. Since measurements of surface exchange rates are limited in their temporal and spatial coverage, extrapolation to other locations and times is usually needed. Detailed understanding of how exchange rates depend on prevailing environmental conditions will greatly facilitate this extrapolation. The ultimate goal of studying surface exchange is to understand the basic biogeochemical mechanisms that control the exchange processes. A full discussion of these issues, however, is beyond the scope of this work. In the following discussions, the emphasis will be on the phenomenological aspects of surface exchange.

Discussion of the behavior of different chemical species in the troposphere necessarily involves consideration of both chemical and physical aspects of the air-surface system, and sometimes biological factors as well. The discussion will use commonly accepted descriptions of different parts of the atmosphere. The air in closest contact with the surface forms a constant flux layer, called the surface layer, some tens of meters thick, in which there is little flux divergence. This constant flux layer is the lowest part (less than about 10%) of the planetary boundary layer (PBL), which is typically 1 to 2 km deep in daytime, 100 to 500 m deep at night over land, and 500 m to 1 km deep over the ocean. The PBL is that part of the lower troposphere that responds to changes at the earth's surface within a few hours and consequently over land exhibits a pronounced diurnal cycle of vertical mixing. During the daytime, convection causes strong mixing, and the PBL is often called the convective boundary layer (CBL). At night, vertical mixing is relatively weak, shallow, and intermittent, and the PBL is often called the nocturnal boundary layer (NBL). The structures of these various layers vary with terrain, latitude, seasons, etc., in ways that complicate the overall behavior of trace species and inject a strong meteorological component into any description of species concentrations, as well as of the change of species fluxes with height, called flux divergence.

Flux divergence plays a crucial role in studying the budgets and distribution of many trace chemical species. For example, flux divergences of species like NO_x and O_3, whose concentrations can differ greatly between the boundary layer and the free troposphere, need to be estimated in order to evaluate their budgets. For the most part, however, flux divergence measurements will not be discussed in great detail since the techniques for measuring flux by eddy correlation apply equally well to multiple levels, as required for flux divergence estimates, and to a single level as required for measuring surface exchange. Other than eddy correlation, flux measuring techniques that can be used for estimating surface exchange are, in general, not applicable for measuring flux divergence.

Oxidant and Odd Nitrogen Group

The nonradical oxidants O_3 and H_2O_2 and the family of odd nitrogen compounds, including NO, NO_2, NO_3, N_2O_5, HNO_3, HNO_2, PAN, and NH_3, play a key and closely interconnected role in the oxidative state of the atmosphere. Because the chemistry of these species is so closely interrelated, it is convenient to consider them together as a family.

Table 1.1
Estimated Photochemical Lifetimes (in Summer)
of O_3, H_2O_2, NH_3, and NO_y

LIFETIME	REGION (1) Tropical marine boundary layer	(2) Rural continental boundary layer	(3) Upper troposphere
Greater than 1 day	O_3, H_2O_2, HNO_3, NH_3	Same as (1)	Same as (1) plus PAN, N_2O_5, other organic nitrates, NH_3
1 hour to 1 day	NO_x, NO_3, some organic nitrates	Same as (1)	Same as (1) plus NO_3, N_2O_5, NO_2
10 min. to to 1 hour	PAN, some organic nitrates, HNO_2*	Same as (1)	None
less than 10 min.	NO, NO_2*, and NO_3*	Same as (1)	Same as (1)

*During the daytime

Table 1.2
Estimated Lifetimes of O_3, H_2O_2, NH_3, and NO_y for Incorporation into
Cloud Water and/or Aerosols

LIFETIME	REGION (1) Tropical marine boundary layer	(2) Rural continental boundary layer	(3) Upper troposphere
Greater than 1 day	PAN, NO_x, O_3, organic nitrates	Same as (1)	Same as (1) plus H_2O_2, HNO_4, N_2O_5, NO_3, HNO_3, and NH_3
1 hour to 1 day	None	H_2O_2, N_2O_5, NO_3, HNO_2, HNO_3, NH_3	None
10 min. to to 1 hour	H_2O_2, N_2O_5, NO_3, HNO_2, HNO_3, NH_3	None	None
less than 10 min.	None	None	None

The major precursors of ozone can be divided into two groups: NO_x (i.e., NO + NO_2), and hydrocarbons and CO. Since CO and CH_4 are readily available in the troposphere, NO_x usually is the rate-limiting ozone precursor. The distribution of NO_x is very inhomogeneous (see Fehsenfeld et al., 1988), as expected from its short photochemical lifetime and highly localized sources. As a result, the ozone production rate should be a very strong function of location.

Table 1.1 gives a list of photochemical lifetimes of ozone, H_2O_2, NO_y species, and NH_3, while Table 1.2 gives the estimated lifetime for the loss of these compounds by incorporation into cloud water and aerosols. The lifetimes of these species range from less than ten minutes to more than a day. Therefore, their distributions and exchange fluxes depend on transport processes of various time scales.

We need to consider here not only surface exchanges but also exchanges between the boundary layer and the free atmosphere; except for a few highly reactive species that originate from surface emissions, boundary layer concentrations of trace chemical species are determined by both interaction with the surface and entrainment of air from the free atmosphere. This is particularly true in studying the global distributions and budgets of O_3, H_2O_2, NO_y species, and NH_3.

Exchange of boundary layer air with the free atmosphere takes place through a variety of mechanisms. On a large (vertical) scale, convective clouds can transport boundary layer air up to near the top of the troposphere within a few minutes and can also bring air from the free atmosphere down to the surface in evaporation-driven downdrafts. On a small scale, both shear and convection can generate turbulence to overcome the static stability of the free atmosphere and cause entrainment of air into the boundary layer.

Since the chemical lifetimes of H_2O_2, NO_x, and NH_3 are less than or comparable to the residence time of air in the boundary layer, the amount of these species exchanged between the boundary layer and the free troposphere may be considerably less than the amount introduced into the PBL. In addition, chemical processing in the PBL serves to convert NO_x to a variety of other NO_y species. Thus, both theoretical and experimental studies should be made to assess this exchange for O_3, NO_y, and NH_3.

A complication for measuring the emission or deposition flux for species such as NH_3, NO_x, and amines (Farquhar et al., 1983), and perhaps also for other gases, is that a compensation point exists, a non-zero gas concentration in the leaf air spaces, which is in equilibrium with metabolites in plant cells. If the ambient concentration exceeds the compensation point, the gas is taken up by the plant from the atmosphere, but if the ambient concentration is less than the compensation point, the gas is emitted to the atmosphere. If enclosure techniques (see Chapter 2) are used to estimate the flux of such chemical species, a correct estimate of the gas flux depends on maintaining gas concentrations in the air within the enclosure very close to ambient. "Closed" enclosure systems are thus unsuitable, and "open" systems will require large ventilation rates, so that leaf boundary layer resistances will be much smaller than stomatal resistances.

Emission rates of N_2O are relatively small compared to those of NH_3 and NO_y (Keller et al., 1986). Natural sources are likely to be the primary contributor, although there is probably some anthropogenic contribution. The only known N_2O sinks are in the stratosphere; surface deposition of N_2O is negligible.

Sources of NO_y, O_3, and H_2O_2

Table 1.3 lists the important sources and sinks of NO_x. Most of the sources are on land and near the surface. Anthropogenic sources appear more important than natural sources, especially in winter, when there are fewer natural sources. Emissions of NO_x are primarily in the form of NO. Once emitted, NO is oxidized quickly to a mixture of NO and NO_2 in photochemical equilibrium, and then to other reactive nitrogen species, such as HNO_3, PAN, NO_3, and N_2O_5. As pointed out by Lenschow and Delany (1987), the rapid photochemical reactions involving NO, NO_2, and O_3 have a considerable impact on their flux and concentration profiles in the surface layer. Figure 1.1 shows a simplified reaction scheme of nitrogen species; a discussion of these reactions and time constants can be found in Logan (1983).

The emission rate of NO_x from soils has been measured primarily by the enclosure technique, as discussed by Galbally (1985) and as summarized in a recent report of the World Meteorological Organization (WMO, 1986; see Chapter 3). Results are summarized in Table 1.4, updated from the WMO report.

Recent comparisons of the enclosure technique and a local budget technique indicate that the methods give similar results (Parrish et al., 1987; Kaplan et al., 1988). The budget technique relies on the fact that at night the reaction of NO with O_3 is the dominant removal process for NO and that atmospheric reactions reforming NO from NO_2 are negligible. Hence, the net flux of NO from the soil must balance the total column loss of NO by reaction with O_3, which may be calculated from vertical profiles of NO and O_3 at night. At least one study of soil emissions has employed the eddy-correlation technique (Delany et al., 1986).

The majority of NO flux measurements have been at mid-latitudes. As discussed in Chapter 3, emission rates measured with enclosures are highly variable, averaging about 1–2 $\times$ 10^{-12} kg N $m^{-2}s^{-1}$ at mid-latitudes, while the few studies in the tropics give values of 8–11 $\times$ 10^{-12} kg N $m^{-2}s^{-1}$, at least for dry soils.

Table 1.3
Global Budget of $NO_x = NO + NO_2$*

SOURCES	Tg N yr^{-1}
Fossil fuel combustion	21 (14–28)
Biomass burning	12 (4–24)
Lightning	8 (2–20)
Microbial activity in soils	8 (4–16)
Oxidation of ammonia	0–10
Oceans	< 1
Stratospheric input	~ 0.5
TOTAL	25–99
SINKS	
Wet deposition	12–42
Dry deposition	11–22
TOTAL	23–64

*Logan, 1983

Emission rates increase with increasing soil temperature and depend also on vegetative cover, soil type, water content, and fertilization. Soils act as both a source and a sink for NO_x, so appropriate care must be taken when determining NO fluxes in field conditions, as discussed by Galbally et al. (1985).

It is of interest to compare the magnitude of the soil source of NO_x with typical emission rates from combustion of fossil fuels. Emissions of NO_x in the U.S. have been estimated by the Environmental Protection Agency (1986), with spatial resolution of 20 km × 20 km. The local anthropogenic source clearly dominates the soil source in over 90% of the eastern U.S., while the soil source is larger than the anthropogenic source in most of the western U.S. Evidently combustion of fossil fuels provides the major source of NO_x over the industrialized regions of Europe, Asia, and North America.

An observational study has been conducted in the Amazon Basin during the dry season (the Amazon Boundary Layer Experiment [ABLE–2A]); preliminary results are discussed in a special issue of *J. Geophys. Res., 93*, 1349–1624. This experiment has provided new insights into the production of NO by biomass burning in a tropical region (Andreae et al., 1988b). The yield of NO with respect to CO_2 in fresh plumes was 0.51×10^{-3}, a factor of ten higher than the value in haze layers about one day old. Previous aircraft observations of large-scale biomass burning emissions in central Brazil (Crutzen et al., 1985a and b) showed that the ratio NO_x/CO_2 in aged fire fume (when fresh plumes were specifically avoided) was $\simeq 1.9 \times 10^{-3}$. Apparently NO_x is oxidized rapidly to HNO_3, PAN,

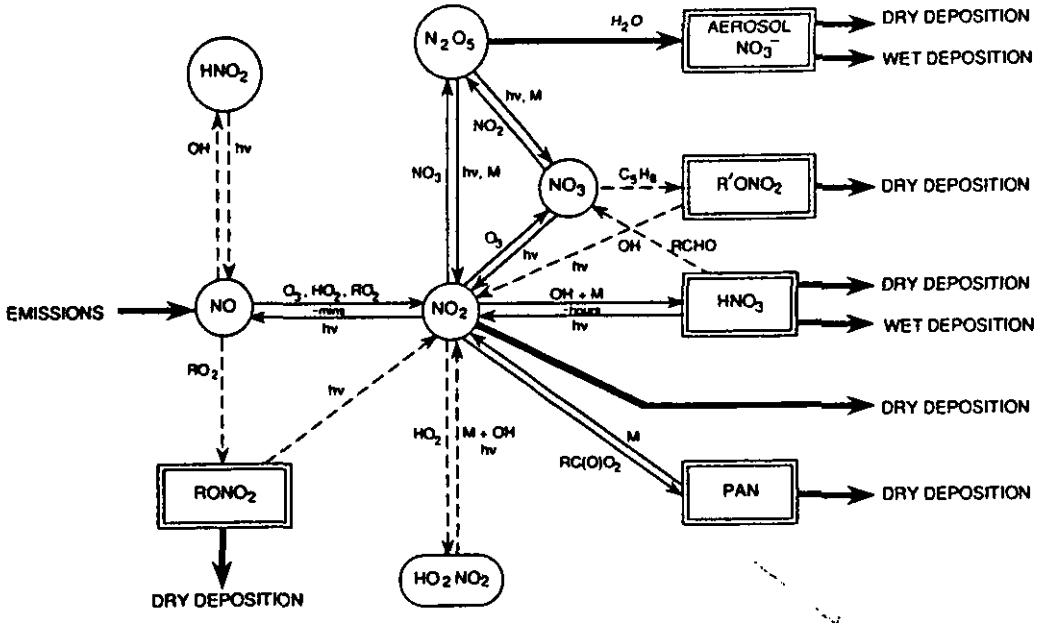

Figure 1.1. Simplified reaction scheme for nitrogen oxides in the atmosphere based on Logan (1983).

Table 1.4

Measurements of NO Emissions from Soils

Surface Type	*Flux* kg N m^{-2} s^{-1} × 10^{12}	*References*
Ungrased pasture (average)	1.6	Galbally and Roy, 1978
Grased pasture (average)	3.5	
Grased pasture (range)	−50	Galbally and Roy, 1981
Fertilised grass (weighted annual average)	1.9	Johansson and Granat, 1984
Unfertilised barley (weighted annual average)	0.6	Johansson and Granat, 1984
Cropland (range)	0.1 to 62	
Unfertilised forest soil		Johansson, 1984
(median)	0.3	
(range)	0.1 to 0.8	
Bare unfertilised soil, Finthen (average)	2.2	Slemr and Seiler, 1984
(range)	−5.8 to 14.2	
Bare unfertilised soil, Utrera (range)	−2.2 to 107	Slemr and Seiler, 1984
Crested wheat grass		Delany et al., 1986
(daily mean)	7	
(range)	−9.3 to 28	
Ungrased grassland		Williams et al., 1987
(mean: Aug–Nov, 1985)	3	
(range)	0.028 to 65	

Surface Type	*Flux* kg N m^{-2} s^{-1} × 10^{12}	*References*
Terra firma forest, Brasil		Kaplan et al., 1988
(mean: enclosure)	10.2	
(mean: vertical gradient)	12.6	
(range)	9.2 to 16	
Burned semiarid		Anderson et al., 1988
chaparral, California (mean)	31[α]	
(range)	6 to 101[α]	
Unburned semiarid		Anderson et al., 1988
chaparral, California (mean)	13[α]	
(range)	0 to 35[α]	
Fertilised corn, 5–30 day		Anderson and Levine,
average[β], Virginia (mean)	25	1987
(range)	6 to 67	
Soy, fertilised 3 months		Anderson and Levine,
prior to study, summer		1987
average, Virginia (mean)	0.7 to 9.4	
Unfertilised grass,		Anderson and Levine,
Virginia (mean)	3	1987
(range)	(0.003 to 9.0)	
Wheat, dry season July,		Anderson and Levine,
Colorado (mean)	2	1987
(range)	0.001 to 6.1	
Wheat, dry season July,		Anderson and Levine,
irrigated Colorado (mean)	10	1987
Wheat, wet season May,		Anderson and Levine,
Colorado (mean)	2.8	1987

[α] Measurements of NO fluxes were made during July and December 1986 at times ranging from 1000 to 1700 LT, at both dry and irrigated sites.

[β] Measurements were made starting 5 days after fertilization and continued for 25 days.

or nitrates in the tropical environment. Background concentrations of NO over the Amazon region increased by about 25% during the month-long expedition, as burning activity increased within and to the south of the study region (Torres and Buchan, 1988). Thus, while biomass burning was the dominant source of NO_x in the vicinity of fires and within plumes, it appeared that emissions from soils provided the major source in the mixed layer and in the convective cloud layer. Andreae et al. (1988b) used the ABLE-2A data to estimate that the global source of NO_x from biomass burning was 7.6 Tg N yr^{-1}, about 2/3 of the estimate given in Table 1.3. The latter figure was based on estimates of the nitrogen content of various biomass fuels, assessments of the extent of burning, and the assumption that 25% of fuel nitrogen is converted to NO.

Elevated concentrations of NO were observed in the vicinity of electrically active clouds over the Pacific Ocean during the first Chemistry Instrumentation Test Experiment (CITE-1) expedition (Davis et al., 1987; Ridley et al., 1987). Chameides et al. (1987) used these data in combination with estimates of the mass flux of air through convective clouds to estimate a global source for NO_x from lightning of 7 Tg N yr^{-1}. This estimate is very similar to that given in Table 1.3, which results from ground-based observations of NO_2 from lightning and satellite data for the total number of lightning flashes per year. The good agreement for the independent methods is remarkable, since both are based on very limited observations of NO_x production by electrical activity.

Table 1.5
Tropospheric NO_x Distributions in the Planetary Boundary Layer (PBL) and Above*

Regions	NO_x (ppbv)
Industrialized PBL	0.5 – 10
Oceanic PBL (0 ~ 2 km)	0.001 – 0.01
Clean continental PBL	0.05 – 0.2
Biomass burning PBL	0.5 – 10
Free troposphere (2 ~ 12 km)	0.02 – 0.2

*Fehsenfeld et al., 1987

Table 1.5, adopted from Fehsenfeld et al. (1987), gives typical observed NO_x levels in five major regions of the troposphere and reflects our current knowledge of the distribution of NO_x sources. The inhomogeneity in NO_x distributions implies that some regions act as ozone sources while others act as ozone sinks (Liu, 1988). The net ozone production (or loss) rates for these regions are shown in Table 1.6. In steady-state conditions, the net ozone production (or loss) equals the flux divergence in a particular region, and the estimated flux divergences are comparable to the stratospheric flux divergences and the surface deposition of ozone. This emphasizes the importance of measuring ozone flux divergence as well as surface deposition.

Table 1.6 shows that ozone production in the free troposphere also has a significant impact on the global ozone budget; yet the sources of free tropospheric NO_x, which plays an essential role in free tropospheric ozone production, are poorly understood. In addition to the contribution from industrial regions, the large biomass fires in the tropics also contribute to the production of ozone on a global scale (Delany et al., 1985). In order to evaluate the impact of anthropogenic activities on tropospheric ozone, the vertical flux divergences of NO_x, PAN, and other reactive nitrogen species emanating from the boundary layer in industrialized regions must be measured.

The ozone budget in the winter half of the year and the seasonal variation of ozone are not understood. This may have important implications for assessing the role of anthropogenic emissions on ozone concentration fields and for estimating possible adverse effects on ecosystems by exposure to high ozone concentrations. Measurements of surface exchange rates and flux divergences of ozone and its precursors in the winter season will resolve some of the key questions involved.

H_2O_2 is produced in both gas-phase and aqueous-phase chemical reactions that involve odd hydrogen species. Like ozone, H_2O_2 formation depends strongly on the distributions of NO_x and hydrocarbons. The photochemical lifetime of H_2O_2 is relatively short—about two days in summer at mid-latitudes. As a result, we expect considerable spatial and temporal variation in the distribution of H_2O_2. Therefore, as in the case of ozone, flux divergence plays a major role in the budget and distribution of H_2O_2.

Deposition of NO_y, O_3, and H_2O_2

Wet and dry deposition are the major sinks for reactive nitrogen species. Soluble species such as HNO_3, NO_3, and N_2O_5 are readily scavenged by precipitation. Ehhalt and Drummond (1982) and Logan (1983) estimate that more than half of the total loss of reactive nitrogen species occurs through wet deposition. Huebert and Robért (1985) have found virtually no surface resistance to HNO_3 exchange from the atmosphere to grass; under these conditions, its deposition is determined by aerodynamic resistance. In some circumstances, HNO_3 deposition may be controlled by phase equilibria (Brost et al., 1988; Huebert et al., 1988). The same can be expected for N_2O_5, which is readily converted to HNO_3 in the presence of surface moisture.

Deposition velocities (v_d—the ratios of surface fluxes to air concentrations at some reference level, typically 2 m height) for NO_2 in the range of 0.3–0.8 cm s^{-1} have been inferred for cement, soil, grass, and agricultural crops from field and laboratory studies,

Table 1.6.

Net Ozone Production or Loss in Summer from Various Regions Averaged over Each Hemisphere and Compared with Stratosphere O_3 Flux

	Net Production or Loss			
	NH		SH	
	(kg m^{-2} s^{-1}) $\times 10^{+12}$	(cm^{-2} s^{-1}) $\times 10^{-10}$	(kg m^{-2} s^{-1}) $\times 10^{+12}$	(cm^{-2} s^{-1}) $\times 10^{-10}$
Free troposphere $\geq$ 2 km	40	5	20	2.5
Industrial areas	8–24	1–3	4–12	0.5–1.5
Oceanic boundary layer	–36	–4.5	–36	–4.5
Clean continental boundary layer	–44	–5.5	–8	–1
Biomass burning areas	1.6	0.2	1.6	0.2
Stratospheric flux	56	7	32	4

while values for NO are considerably lower, $< 0.1 - 0.2$ cm s^{-1} (Judeikis and Wren, 1978; Bottger et al., 1978; Galbally and Roy, 1981; Varhelyi, 1980). Wesely et al. (1982b) investigated loss of NO_x over a soybean field, using an eddy-correlation technique. They reported a maximum deposition velocity for NO_2 of 0.6 cm s^{-1} during the day, with a minimum value of 0.05 cm s^{-1} at night during windy conditions. These, however, are uncertain due to the nonspecific nature of their NO_2 measurements. Garland and Penkett (1976) reported deposition velocities for PAN of 0.25 cm s^{-1} over grass and soil.

The deposition of NO and NO_2 on water surfaces should be negligible because of the low solubility of these chemical species (Lee and Schwartz, 1981). There is no published measurement of the deposition velocities for NO, NO_2, or PAN under winter conditions. Since the photochemical lifetimes of NO_x and PAN become longer in winter, dry deposition may play an important role in their budgets, and measurement of the deposition of NO_x and PAN for winter conditions should be a high priority.

Dry deposition of particulate NO_3^- depends very much on the size distribution of the particles involved, or, in some cases, on particle-gas interconversion (Brost et al., 1988; Huebert et al., 1988). (In both the continental and marine boundary layers, there may be situations in which aerosol nitrate evaporates and deposits as HNO_3 vapor.) Coarser particles tend to have larger gravitational settling velocities, while fine particles are transported much like gases. There are serious shortcomings in our understanding of the dry deposition of particles. This problem will be discussed in Chapter 4.

Considerable work has been done on measurements of deposition of ozone over various surfaces for summer daytime conditions (e.g., Aldaz, 1969; Galbally and Roy, 1980; Lenschow et al., 1981, 1982; Wesely et al., 1981; Wesely, 1983; Greenhut, 1983; Cobeck and Harrison, 1985; and Kawa, 1988). Over land, daytime deposition velocities range from 0.2 to 2 cm s^{-1} during the summer. Photosynthetically active vegetation has a relatively small surface resistance to ozone. Measurements over oceans and fresh water (Galbally and Roy, 1980; Wesely et al., 1981; Lenschow et al., 1982; Kawa, 1988), although limited, are sufficient to demonstrate that surface resistances are large and result in deposition velocities in the range of 0.02 to 0.1 cm s^{-1}. Measurements under nighttime conditions are relatively few. However, this may not be a serious problem for evaluating the ozone budget, because deposition at night is limited by transport processes. As a measurement strategy for ozone deposition, the highest priority probably should be given to measurements under winter conditions.

Both wet and dry deposition are significant sinks for H_2O_2. There have been few measurements of either, because reliable instruments for measuring H_2O_2 have been available only recently (Heikes et al., 1986).

Ammonia

Ammonia, the main nitrogen-containing compound in primordial earth's atmosphere, is now present only in trace amounts. It is unique among atmospheric trace species as the only basic gaseous species present in significant concentrations (typically 0.1 to 19 ppbv [7.7×10^{-11} to 1.5×10^{-8} kg m^{-3} STP]) near ground level. For this reason, its accession to the atmosphere, the dispersion and transformations it undergoes there, and its subsequent deposition are of great interest in many earth sciences, including meteorology, atmospheric chemistry, soil science, agronomy, and ecology.

Concentrations in "clean" air over land are typically in the range of 1.3 to 13 ppbv (10^{-9} to 10^{-8} kg m^{-3} STP) (Ayers and Gras, 1980), although concentrations in rural areas with much livestock production may be very much higher, up to 330 ppbv (2.5×10^{-7} kg m^{-3} STP) as a daily average (Vermetten et al., 1985). Concentrations in clean air over the oceans are quite low, < 0.13 ppbv (10^{-10} kg m^{-3} STP) (Ayers and Gras, 1980).

A precursor of the chemical subunits of early life, ammonia is now formed in nature from the biological degradation of proteins in soil organic matter, plant residues, and animal wastes. Smaller amounts are also emitted from fertilizer breakdown and from industrial and combustion processes.

There is considerable guesswork in published estimates of NH_3 emissions. Galbally (1985) discusses some of the problems. Among more recent estimates are those made by Crutzen (1983) in an up-date of an earlier ammonia budget of Söderlund and Svensson (1976). Crutzen's estimates of annual global emissions are:

Biomass burning	< 60 Tg N/year
Emissions from natural fields	< 30 Tg N/year
Excreta from domestic animals	10 to 20 Tg N/year
Coal burning	4 to 12 Tg N/year
Excreta from wild animals	2 to 6 Tg N/year
Emissions from fertilized fields	< 3 Tg N/year

The biggest source, biomass burning, is probably the most uncertain, so it is important that its magnitude be verified. Vines et al. (1971) were unable to detect NH_3 in the smoke of bushfires, small fires in the laboratory, or large forest fires. They suggest that NH_3 that formed during the pyrolysis of nitrogen compounds would probably be oxidized to water and molecular nitrogen at the flame temperatures prevailing in bushfires. Crutzen, on the other hand, attributes to Söderlund and Svensson (1976) the statement that NH_3 is a surprisingly stable compound in combustion systems, and Galbally (1985) expresses the view that a significant fraction of the nitrogen must be volatilized as NH_3 during the heating and burning of plant material. Recent measurements of NH_3 emissions from laboratory-scale biomass fires yield an estimate of 3.2 Tg N (NH_3) yr^{-1} for the global annual emission (Andreae, personal communication, 1989; data from W. M. Hao, Max Planck Institute for Chemistry, Mainz, FRG).

The next largest NH_3 source suggested by Crutzen is release from natural (unfertilized) fields, up to 30 Tg N yr^{-1}. As discussed by Crutzen and by Galbally (1985), this is difficult to estimate because soils and plants can be either sources or sinks. Crutzen's estimate is based on a model of NH_3 production and transport in soils developed by Dawson (1977). The model predicts that the concentration of NH_3 contained in air within the soil is always very much larger than in the free atmosphere (by a factor of between 70 and 300), so that the soil is always a source of atmospheric NH_3.

Malo and Purvis (1964) and Hannawalt (1969), however, concluded from laboratory and field experiments that soils could be substantial sinks for atmospheric NH_3. Although the atmospheric concentrations they employed in the laboratory and measured in the field (39 to 78 ppbv [3 to 6×10^{-8} kg m^{-3} STP]) were rather larger than normal ambient values, they were, nevertheless, still much smaller than the values Dawson predicts for soil.

Dawson's model also neglects the possible absorption of NH_3 from air as it diffuses through the canopy space. Hutchinson et al. (1972) have shown that plants can absorb NH_3 gas by diffusion through stomata, and Denmead et al. (1976) found strong evidence for the existence of a closed NH_3 cycle in plant canopies, whereby NH_3 released from the decomposition of litter at the soil surface is reabsorbed by the foliage above. In other work, Denmead et al. (1978) found that at normal concentrations (up to 13 ppbv [10^{-8} kg m^{-3} STP]), atmospheric ammonia was taken up by a corn crop (plant plus soil) when the soil surface was dry, but sustained NH_3 losses from the crop occurred when the surface was moist. They suggest that the net exchange is a balance between absorption by the plants and emission from the soil. The latter is strongest when water is being evaporated. Crutzen (1983) suggests that a significant release of NH_3 to the atmosphere could occur in early spring, when the soil is moist, fresh vegetation is not well developed, but dead material on the ground is abundant and the soil is being heated strongly.

Whether plants themselves lose or gain ammonia appears to be controlled by the NH_3 compensation point. Farquhar et al. (1980) have found that for the

plant species they examined, the compensation point is close to normal clean-air concentrations, although it increases with increasing temperature, partly because of the effects of temperature on the equilibrium vapor pressure of NH_3 solutions and increases also during senescence, presumably because of changes in plant metabolism (Farquhar et al., 1979). The temperature dependence has been suggested as a reason for the apparently higher atmospheric concentrations of NH_3 in tropical regions.

The fact that compensation points are normally close to ambient concentrations makes considerable sense. Plants with higher compensation points would be at an ecological disadvantage. Given all this, it seems that in normal clean air, atmospheric exchange of NH_3 will be of small consequence to the nitrogen budget of many agricultural crops, except during periods of elevated temperature or in senescence, but atmospheric exchange may be more important in natural communities with smaller nitrogen turnovers.

Excreta from domestic animals is the next largest source on Crutzen's list and the one that many believe may be the largest. Crutzen's estimate is based on average rates of urea excretion in urine and feces by livestock, and an assumption that 30% of the nitrogen in the urea would be volatilized as NH_3. Estimates of the latter range from 10 to 45% (Lenhard and Gravenhorst, 1980).

From aircraft measurements of the concentration of NH_3 and NH_4^+ in the air at 100 m and 700 m above a rural area in western Germany, Lenhard and Gravenhorst (1980) estimated upward fluxes of NH_3 and NH_4^+ and concluded that these could be maintained entirely by NH_3 volatilization from domestic animal excreta, again assuming that 30% of the excreted urea nitrogen is volatilized as NH_3. Galbally et al. (1980) also estimated that the major emissions of NH_3 to the atmosphere in Australia were from this source, some 70%. The most detailed estimates currently available are those of Buijsman et al. (1987), who calculated that 81% of the total anthropogenic NH_3 emissions in Europe were from livestock wastes. They also estimated that natural emissions of NH_3 in Europe (from uncultivated land areas) contribute only 0.6 Tg N yr^{-1}, compared with livestock emissions of 4.3 Tg N yr^{-1} and total anthropogenic emissions of 5.3 Tg N yr^{-1}.

Other minor sources include coal burning, excreta from wild animals, emissions from fertilized fields, and industrial emissions (< 1 Tg N yr^{-1}). Apart from excreta from wild animals, these are the best-documented sources, but, even so, there are still some unknowns. In calculating emissions from fertilized fields, for instance, Crutzen takes the NH_3 contribution as about 5% of the annual fertilizer use of almost 60 Tg N, but published estimates of NH_3 loss from fertilizer application range from 0 to 50%, depending on fertilizer type, soil, weather conditions, and methods of application.

Two trends in modern agricultural practice are worth noting here. One is the increasing use of urea as a fertilizer. Buijsman et al. (1987) suggest an emission factor of 10% for urea, which is twice Crutzen's figure. The second is a shift to minimum cultivation practices, which means that more fertilizer is spread on the soil surface, where its gaseous decomposition products can be easily lost to the atmosphere, instead of being incorporated within the soil, where released NH_3 can be quickly fixed by the soil exchange complex. Additionally, the use of more nitrogen fertilizers in developing countries, where agricultural practices are often inefficient, will probably lead to higher NH_3 emissions.

Ammonia is returned to the earth's surface as NH_3 and NH_4^+ very efficiently by both wet and dry deposition, so that the majority of emitted NH_3 is probably deposited in the vicinity of its sources. While the flux densities of nitrogen from these sources (typically, 1 to 2 × 10^{-3} kg N m^{-2} yr^{-1} [3.2 to 6.4 × 10^{-11} kg N m^{-2} s^{-1}]) compared with fertilizer applications of ~10^{-2} kg N m^{-2} yr^{-1} (3.2 × 10^{-10} kg N m^{-2} s^{-1}) are relatively small in comparison with inputs of nitrogen to fertilized fields, they are certainly of consequence in the nitrogen balance of natural ecosystems.

A new environmental effect of atmospheric NH_3 is now emerging, particularly in regions of high NH_3 turnover, as in Europe (Buijsman et al., 1987). Serious soil-acidifying effects have been observed, which could be attributed to wet deposition of NH_4^+ and dry deposition of NH_3 and ammonium aerosols.

The role of the oceans is largely unknown. Some measurements of NH_3 in marine air by Ayers and Gras (1980) suggest that the atmospheric concentration is close to the equilibrium gas concentration to be expected for seawater, which suggests that the oceans are unlikely to be net sources or sinks. At present, there are likely too few measurements of NH_3 in surface air over the oceans or in ocean surface waters to decide this question (Galbally, 1985).

Sulfur Group

Both natural and anthropogenic sources contribute to the global sulfur budget. Anthropogenic sulfur emissions are dominated by the release of SO_2 from fossil-fuel burning. Several authors have recently reviewed these emissions and presented detailed source allocations (e.g., Möller, 1984; and Cullis and Hirschler, 1980); the estimates fall into a relatively narrow range of about 70 to 100 Tg S yr^{-1}.

Various attempts to derive a global atmospheric budget for sulfur have suggested that natural emissions of a magnitude comparable to man-made emissions

are necessary to balance this budget (for a review, see Frency et al., 1983). However, since the calculations of natural emissions from the difference between anthropogenic emissions and total deposition fluxes involve very large uncertainties, they cannot be expected to provide a meaningful estimate.

This section is an overview of the processes that result in the natural emissions of sulfur species and provides, where possible, estimates of these fluxes. Only fluxes of natural gaseous sulfur species are given extensive coverage here. For detailed discussions of other emissions, such as sea salt sulfate and volcanic emissions, the reader is referred to the reviews by Andreae (1985, 1986).

Production of Volatile Biogenic Sulfur Compounds

Sulfur is an essential element to biological organisms. Two biological pathways lead from sulfate (the major sulfur source for almost all organisms) to reduced sulfur compounds: assimilatory and dissimilatory sulfate reduction. Volatile organosulfur compounds are produced from nonvolatile sulfur metabolites in biota either through the formation and release of volatile sulfur metabolites in healthy living cells or as a consequence of decomposition. The most important product released from live cells, especially by plants, is dimethylsulfide (DMS), which is discussed later in some detail. The major pathway to the formation of H_2S, however, is through dissimilatory sulfate reduction. Under favorable conditions, the rate of sulfate reduction to H_2S can be quite high, on the order of several tens of $\mu g\ m^{-2}\ s^{-1}$. However, this process occurs only when a mixing barrier prevents oxygen from entering the system. (The escape of H_2S from the system is, of course, limited by the same barrier.) Furthermore, in the presence of oxygen, H_2S can be consumed by bacteria in a layer only a fraction of a millimeter thick. Consequently, the large amounts of H_2S that are produced in the coastal and marine environment are not usually transferred to the atmosphere (Andreae, 1984). Only a small fraction of the H_2S produced can escape under exceptional conditions in shallow water. H_2S emissions from the marine environment are, therefore, limited to such near-shore environments as estuaries and salt marshes.

Table 1.7

Summary of Biogenic Sulfur Emission Measurements*

Source	Location (State)	Month (1985)	Number of Samples	Geo. Mean Emission	Mean Sample Temperature (°C)
Soils				kg S $m^{-2}s^{-1}$ $\times 10^{14}$	
Inceptisol	ID	3, 4, 9, 10, 11	17	4.5	10.9
Entisol	ID	3, 4, 5, 10	11	16.9	11.9
Alfisol	ID	5, 6, 10	15	26.6	
Mollisol	IA	7	15	18.4	38.4
Histisol, bare	OH	7	18	341.0	32.9
Tidal shore	NC	8	8	374.0	36.3
Saline marsh (with grass)	NC	8	25	580.0	32.7
Salt water	NC	8	5	51.6	31.4
Fresh water	NC	8	4	264.0	29.6
Crops					
Oats (with soil)	IA	7	11	1.6	35.4
Misc. vegetables (with soil)	OH	7	6	123.7	29.3
				kg S $kg^{-1}s^{-1}$ $\times 10^{14}$	
Corn	IA, OH	7	36	103.0	28.9
Soybeans	IA	7	16	210.0	32.8
Alfalfa	WA	9	6	179.0	22.4
Trees					
Deciduous	IA, OH, NC	7, 8	55	47.1	29.5
Coniferous	NC	8	13	31.1	29.2

*Lamb et al., 1987

Sulfur Emissions from Continental Ecosystems

Due to the lack of representative data, estimates of the flux of biogenic sulfur gases from terrestrial soils and plants have been highly uncertain, ranging from 3 to 110 Tg S yr^{-1} (Andreae, 1986). Here, we will focus on the results of recent measurements of emissions from freshwater wetlands, inland soils, and terrestrial plants.

The concentrations of dissolved volatile sulfur compounds in freshwater bodies tend to be much lower than those in the surface layer of the oceans (Adams et al., 1981; Froelich et al., 1985; Iverson et al., 1989). However, based on measurements of DMS concentrations in water from freshwater wetlands in Ontario, Nriagu et al. (1987) recently proposed a DMS emission rate of 2.5×10^{-12} kg S m^{-2} s^{-1} for such ecosystems and suggested that H_2S emissions of a similar magnitude may be occurring. These fluxes may, however, be overestimated, since the exchange coefficient appropriate for the hydrodynamic regime of the bog is not known and a rather high value was assumed. It is also likely that very high sulfate loading from anthropogenic pollution may have enhanced sulfur flux from these wetlands. Recent studies in Alaska suggest extremely low emissions of volatile sulfur from bog and tundra ecosystems (Martens, personal communication, 1988).

Adams et al. (1981) determined the flux of sulfur gases from soils in the eastern and southeastern United States. Their flux data showed several orders of magnitude variability between sites and between sampling periods at the same site; for nonsaline soils, they ranged from 6.6×10^{-14} to 1.1×10^{-11} kg S m^{-2} s^{-1}. Most of the flux from inland soils was in the form of H_2S (66%); the rest was COS (13%), CS_2 (13%), DMS (7%), and a trace of DMDS (2%). Delmas et al. (1980) measured an average H_2S flux of 2.2×10^{-12} kg S m^{-2} s^{-1} from oxic lawn soils in France. Jaeschke et al. (1980) found fluxes of H_2S between 3.3×10^{-14} and 3.3×10^{-11} kg S m^{-2} s^{-1} from marshland soils in the Ems River region of northern Germany. Much higher fluxes were estimated from tropical soils in the Ivory Coast by Delmas et al. (1980): 9.7×10^{-12} to 2.8×10^{-11} kg S m^{-2} s^{-1}.

Most recent studies have found much lower flux estimates from soils. In a large study of soil emissions conducted partly at the same sites as those used by Adams and coworkers, values about ten times lower than those reported previously were obtained by Goldan et al. (1987) and Lamb et al. (1987b) (Table 1.7). The differences between these values and those reported previously are believed to be due largely to experimental problems in the older studies. Preliminary results from measurements of soil emissions in wet tropical forests in Brazil during the dry season as follows: $(2.2 \pm 0.2) \times 10^{-13}$ kg S(DMS) m^{-2} s^{-1}, $(2.2 \pm 0.5) \times 10^{-14}$ kg S(CH_3SH) m^{-2} s^{-1} and $(3.7 \pm 1.7) \times 10^{-14}$ kg S(H_2S) m^{-2} s^{-1}. These values give a total flux of short-lived sulfur species of $(2.7 \pm 0.43) \times 10^{-13}$ kg S m^{-2} s^{-1} (Andreae and Andreae, 1988). During the wet seasons, even lower values were observed. However, due to the small number of measurements and sites involved, our ability to extrapolate from these data is very limited.

The emission of sulfur gases from vegetation, including trees, is well established. The emission of H_2S from leaves is light-dependent; it increases strongly with the intensity of light and drops to very low values in the absence of light (Wilson et al., 1978; Filner et al., 1984). Emission of H_2S also increases as a result of root injury, high levels of atmospheric SO_2, and increased levels of soil water sulfate or bisulfite. Based on studies with various crop plants, Filner et al. (1984) estimated a worldwide emission of volatile sulfur from plants on the order of 7.4 Tg yr^{-1}, whereas Winner et al. (1981) estimate ~50 Tg yr^{-1}. Adjusting these values to the leaf areas and biomass values characteristic of tropical forests, fluxes of about 2.7×10^{-12} to 27×10^{-12} kg S m^{-2} s^{-1} can be predicted. Filner et al. (1984) also report the emission of CH_3SH by plants under some conditions. The emission of DMS from trees was observed by Lovelock et al. (1972); a flux of 5×10^{-13} to 10^{-11} kg S m^{-2} s^{-1} is estimated from their data for a forest with a leaf mass of ~2 kg (dry weight) m^{-2}. In a recent study on sulfur gas emissions from plants and soils, Lamb et al. (1987b) found emission fluxes in the range of 10^{-13} to 10^{-12} kg S m^{-2} s^{-1} from various crops and trees. The mean sulfur flux from deciduous trees was 5×10^{-13} kg S m^{-2} s^{-1} during summer conditions (mean sample temperature: 29.5°C). Emissions from soybeans and corn were dominated by DMS, while deciduous trees emitted similar amounts of H_2S and DMS. These fluxes are comparable to or greater than the sulfur gas emission fluxes that have been reported from vegetated inland soils.

Comparison of the emissions of COS from bare and vegetated soils showed that the vegetation canopy was a sink for this gas, reducing the flux of COS from soils to the atmosphere (Goldan et al., 1987; Fall et al., 1988). The uptake of COS by vegetation has been proposed as the major global sink for this compound (Brown and Bell, 1986).

The fluxes of DMS, H_2S, and CH_3SH from the soil/plant system of the Amazon forest were determined during the 1985 dry season by a gradient/flux technique (Andreae and Andreae, 1988). The mean fluxes were 4.2×10^{-13} and 2.2×10^{-13} kg S m^{-2} s^{-1} for DMS and CH_3SH respectively (Andreae et al., 1989a). Since these fluxes are much larger than the observed soil fluxes, most of the sulfur emissions must come from the plant canopy. In the case of DMS,

the vertical profiles through the forest canopy suggested that emission takes place only during the daytime and that the forest canopy is a sink for this species during the night.

If these observations are representative for remote continents worldwide, an assumption which is supported by the existing data for sulfate deposition (Galloway, 1985; Andreae et al., 1989b, and references therein), the biogenic sulfur emission from continents must be near the lower end of the range given in Table 1.10, and emissions from land biota must play a subordinate role in the continental sulfur cycle over the continents worldwide, being overshadowed by marine and anthropogenic sources essentially everywhere.

Emissions from Coastal Wetlands

Emissions of sulfur gases from saline marshes and intertidal areas vary widely between sites, between seasons, and even between days (Aneja et al., 1982; Hansen et al. 1978; Adams et al., 1981; Jaeschke et al., 1980; Steudler and Peterson, 1984; Ingvorsen and Joergensen, 1982; Cooper et al., 1987; DeMello et al., 1987). The results from flux-chamber measurements range from undetectable to nearly 6.3×10^{-8} kg S m^{-2} s^{-1} during peak periods. Typical emission rates for various sulfur species are presented in Table 1.8.

Many of the reported differences are caused by diurnal and seasonal variations. The production of oxygen by photosynthesis leads to rapid oxidation of H_2S in surface layers of intertidal sediments and marshes, thereby preventing most of the H_2S produced in the anoxic zone from escaping into the atmosphere. At night, the anoxic zone moves to the sediment surface, and the emission of H_2S increases by several orders of magnitude (Hansen et al., 1978; Revsbech et al., 1983). COS is produced from organosulfur compounds by photochemical reactions (Ferek and Andreae, 1984). The strong diurnal variability in COS emissions from salt marshes reported by Carroll et al. (1986) may be related partly to the photochemical dependence of the production rate and partly to soil-temperature and tidal cycles.

It is difficult to assign an average value to the flux of volatile sulfur compounds from coastal wetlands. However, even if we were to use a relatively high estimate of 10^{-2} kg S m^{-2} yr^{-1} for the average annual flux and combine it with the total global coastal wetland area of 380,000 km^2, we would obtain a global flux of ~4 Tg S yr^{-1}, which is only a small percentage of the total biogenic emissions.

Emissions from Biomass Burning

The composition of sulfur species emitted from fires is still quite uncertain. It had been assumed that SO_2 was the major product, but H_2S, COS, and sulfate aerosol have also been observed and may be important. The global emission rate for COS from biomass burning has been estimated to be 0.11 Tg S yr^{-1}. Although this is only a minor fraction of the sulfur flux from fires, it is a significant component in the atmospheric cycle of COS (Crutzen et al., 1979).

Sulfur species recently measured in aerosols generated by biomass burning in Brazil suggest that global sulfur biomass emissions may be on the order of 2.6 Tg S yr^{-1} (Andreae et al., 1988b). The differences between the results of these direct measurements and the estimates given above may be due to lower sulfur content of the biomass or to a lower volatilization efficiency.

Table 1.8

Emissions of Volatile Sulfur Compounds from Coastal Wetlands*
In Units of (kg S $m^{-2}s^{-1}$) x 10^{11}

Compounds	Various Saline Wetlands	Salt Marshes	Salt Marshes
H_2S	1.9	1.7	7.6
COS	0.29	—	1.1
MeSH	0.29	≤ 6.0	—
DMS	0.70	2.1	4.8
CS_2	0.38	≤ 0.6	0.6
DMDS	0.03	≤ 2.6	1.1
Total S	3.49	< 35.0	15.0

*Andreae, 1986 (The two columns at right are from different studies.)

Emissions of Volatile Sulfur Species from the Oceans

Bingemer (1984) has made the only measurements of sulfur gas flux from seawater in a chamber system at zero wind speed using the DMS naturally present in seawater. For DMS concentrations of 4×10^{-8} to 9×10^{-7} kg S(DMS) m^{-3}, he found fluxes that compare reasonably well with the predictions from theory. For other gases, however, we have to rely entirely on extrapolations based on relatively poorly developed theories. The uncertainties involved in estimating transfer fluxes with this approach introduce a potential error of as high as a factor of two into the estimates of oceanic sources of most species.

Alternative methods to measure the flux (e.g., eddy correlation or gradient techniques) are difficult. No fast-response sulfur gas sensors suitable for eddy-correlation measurements are yet available for any sulfur gas in the remote atmosphere. Nguyen et al. (1984) have used the gradient method onboard ship by taking samples at different levels above the waterline. Although the results are comparable to the predictions from gas-transfer calculations, they may contain substantial errors because of the influence of the ship on airflow characteristics. Since a realistic wave climate is difficult to simulate inside an enclosure, sulfur-gas fluxes across the air/sea interface have not been measured by this technique. Therefore, in the following discussion of the fluxes of individual sulfur species, predictions are made using the transfer model, which uses gas concentrations measured in seawater and boundary-layer air.

In open ocean waters, DMS is the predominant volatile sulfur compound (Barnard et al., 1982; Andreae et al., 1983; Andreae and Barnard, 1984; Nguyen et al., 1984; Cline and Bates, 1983; Bingemer, 1984). Although other compounds, especially CS_2 and CH_3SH, may also be present in coastal waters (Turner and Liss, 1985), their limited distribution and relatively low concentrations allow for only minor contributions to the global atmospheric sulfur budget. DMS is produced near the ocean surface by phytoplankton from an intracellular biochemical precursor, dimethylsulfonium propionate.

The analysis of large data sets and of the vertical distribution of DMS in the marine water column clearly show that the DMS concentration in seawater is related to the abundance of phytoplankton. Nevertheless, a direct correlation between total plankton abundance and DMS concentration within a given region has not yet been established because of the substantial differences in the DMS output rate of different plankton species (Andreae et al., 1983; Barnard et al., 1982). As Table 1.9 shows, when emissions of DMS from different marine biogeographic regions are compared, emissions from large oceanic regions of relatively low productivity appear to be as important to the global flux as those from localized "hot spots" of high productivity, e.g., upwelling areas.

Based on a large data set from a wide variety of oceanic biogeographical zones, Andreae and Raemdonck (1983) have calculated an average DMS concentration for each zone and a global sea-to-air flux of ~40 Tg S yr^{-1}. This estimate is subject to an uncertainty of about ±20 Tg, most of which derives from the uncertainties involved in using the "stagnant film" model to estimate air-sea transfer. Other researchers have recently published comparable flux estimates based on geographically limited concentration data sets (Nguyen et al., 1984; Bingemer, 1984; Cline and Bates, 1983).

To verify these estimates, it is important to find independent checks on the flux of DMS from the oceans. DMS concentrations of 100 to 300 pptv (2.8×10^{-10} to 8.4×10^{-10} kg DMS m^{-3} STP) are consistently found from a number of measurements in remote marine atmospheres (Andreae and Raemdonck, 1983; Andreae et al., 1985). These concentrations are consistent with the measured reaction rate of DMS with OH and a sea-to-air flux of the same magnitude as estimated above (Graedel, 1979; Chatfield and Crutzen, 1984).

Concentrations of one to a few $\times 10^{-9}$ kg S(COS) m^{-3} of COS are found in surface seawater (Rasmussen et al., 1982; Ferek and Andreae, 1984; Turner and Liss, 1985). Since observed concentrations are almost always higher than the equilibrium concentration relative to the overlying atmosphere, a net sea-to-air flux exists essentially across the entire ocean surface. Using samples collected without considering the diurnal cycle and only separated into coastal and open-ocean values, Rasmussen et al. (1982) estimate a global COS flux from the oceans of 0.3 Tg S yr^{-1}. Based largely on coastal data and interpolation from an observed relationship of DMS and COS, Ferek and Andreae (1984) estimate a global flux of 0.5 Tg S yr^{-1}.

Carbon disulfide in seawater was first found by Lovelock (1974), who measured an average concentration of 4.4×10^{-10} kg S(CS_2) m^{-3} in 35 samples taken from the open Atlantic. Inshore values were about an order of magnitude higher. Recent measurements by Kim and Andreae (1987) have been used to estimate an oceanic CS_2 flux of 0.2 Tg S yr^{-1}, which is small relative to the oceanic DMS flux.

Although H_2S, CH_3SH, and DMDS have occasionally been reported, their concentrations appear to be insignificant relative to other oceanic sulfur emissions. A recent report of sulfur-containing amino acids in the marine boundary layer (Mopper and Zika, 1987) indicates that they and their atmospheric oxidation products could be another significant source of sulfur over the oceans.

Table 1.9

DMS Concentrations and Fluxes for the World Oceans

Biogeographic Region	Area (10^6 km^2)	Mean Conc. (kg DMS m^{-3}) × 10^6	Total Flux (Tg S yr^{-1})
Oligotrophic (tropical/ low productivity)	148	15	6–19
Temperate	83	13	3–10
Upwelling (coastal and equatorial)	86	30	6–22
Coastal/shelf	49	17	3–6
		Mean: 19	Total: 19–54

Summary of Natural Sulfur Emissions

The fluxes of the sulfur compounds SO_2, H_2S, COS, DMS, CS_2, and sulfate are summarized in Table 1.10. Large uncertainties obviously exist in both the chemical speciation and the magnitude of these fluxes. Although the estimated sea salt aerosol flux introduces a very large uncertainty into the total estimate, even after removing this component the range of estimates for the gaseous flux is still 38 to 89 Tg S yr^{-1}.

Clearly, better estimates of sulfur fluxes are needed to reduce this uncertainty. The flux estimates are most sensitive to inaccuracies in the major constituents. Therefore, SO_2, $SO_4^=$ particulates and aerosols, DMS, and H_2S are given the highest priority as species for which precise and accurate flux measurements are needed. Table 1.10 also indicates the most critical study regions for flux measurements.

Deposition of Sulfur Species

Reduced sulfur species are oxidized in the atmosphere to SO_2 and particulate $SO_4^=$. The atmospheric sulfur cycle is completed by the wet and dry removal of SO_2 and $SO_4^=$. On continental scales, the ratio of dry to wet deposition of sulfur appears to be of the order of unity (Shannon, 1981; Galloway et al., 1984).

Dry deposition of SO_2 and particulate $SO_4^=$ has been studied extensively in the industrialized countries because of concern over acid deposition (e.g., Hicks et al., 1987). The deposition of SO_2 on various surfaces has been observed to be moderately rapid, with deposition velocities of 0.3 to 0.6 cm s^{-1} in summer. In winter, the deposition velocity is significantly smaller. The deposition of particles larger than about 2 μm is controlled by gravitational settling. These particles tend to be deposited locally, while smaller particles can be transported over long distances. The average deposition velocity for $SO_4^=$ particles is about 0.1 to 0.5 cm s^{-1} in summer and about half that in winter.

Uptake of COS by various plant species has been observed by Taylor et al. (1983), Kluczewski et al. (1983, 1985), and Goldan et al. (1988). They show that the surface resistance of COS is similar to that of CO_2 under various conditions of controlled illumination, temperature, and CO_2 concentration. This similarity provides a means for estimating global COS uptake by plants. The annual uptake is estimated to be from 0.1 to 0.3 Tg S yr^{-1}. This appears to be the largest global sink for COS (Goldan et al., 1988).

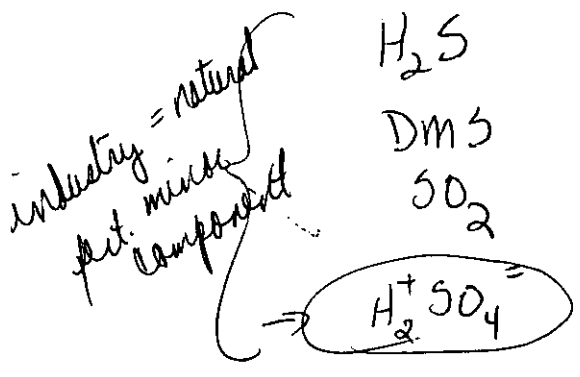

Table 1.10
Estimates of Natural Sulfur Emissions (in Tg S yr^{-1})

	SO_2	H_2S	COS	DMS	CS_2	Sulfate	Other	Total
Sea spray						38.00–320		38.0–320
Dust						3.00–32		3.0–32
Total Particulates						1.42–352		42.0–352
Volcanoes	7.4–9.3	1.0	0.010	—	0.010	< 3	?	10.0–13
Soils and plants	—	3.0–10	0.2–0.6	0.2–4	0.6–0.8	—	1.0	5.0–13
Coastal wetlands	—	1.0	0.1	0.6	0.06	—	0.1	1.9
Biomass burning	2.6	?	0.1	—	?	?	?	≥ 2.6
Oceans (gases)	—	1.6–6.4	0.4	19.0–51	0.3	—	?	35.0–58
Total Gases	10.0–13	6.0–19	1.0–1.3	19.0–54	1.0–1.3	≤ 3	1.0	38.0–89

Carbon Group

The global atmospheric carbon budget is dominated by CO_2, and this aspect of the carbon cycle has been studied intensively for many years (Bolin et al., 1979; Bolin, 1981; Trabalka and Reichle, 1986). Nevertheless, it is sobering to realize that even after considerable effort it is still not possible to adequately reconcile the measured distribution of CO_2 in the atmosphere with the surface exchange that constitutes the major sources and sinks of this gas (see Tans et al., 1989). Nor is it possible to account satisfactorily for the strong, asymmetric meridional gradient of ^{18}O in atmospheric CO_2 (Francey and Tans, 1987). While CO_2 may dominate the carbon budget, it is clear that fluxes of other, much less abundant carbon species play key roles both in the carbon cycle itself and in the broad chemistry of the troposphere. For example, carbon monoxide (CO) is present in the troposphere at an average concentration of about 0.03% of that of CO_2, but the quantity of CO_2 formed each year by the oxidation of CO by OH is significant when compared to the quantity of CO_2 released directly into the atmosphere by the burning of fossil fuels. Naturally occurring nonmethane hydrocarbons (NMHC) are present at concentrations almost two orders of magnitude lower than those commonly observed for CO, but they significantly affect the formation of tropospheric ozone in both rural (Trainer et al., 1987) and urban locations (Chameides et al., 1988). During the atmospheric oxidation of methane (CH_4) and NMHC to CO and CO_2, much of the carbon flux passes through the species formaldehyde, but its concentration in the troposphere is typically less than one part per billion by volume (Dawson and Farmer, 1988). Another organic species that influences the formation of oxidants in the atmosphere is acetone, since it acts as a precursor of peroxyacetylnitrate (PAN), which may then act as a source of reactive nitrogen in the remote troposphere (Arnold et al., 1986).

The following sections, together with Table 1.11, provide a summary of what is currently known about the surface exchange of the key carbon species.

Carbon Dioxide

Carbon dioxide does not play a direct role in the chemistry of the troposphere. Nevertheless, the warming of the earth's surface and troposphere, as well as the cooling of the stratosphere above 20 km, that are likely to result from continuing increases in global CO_2 concentration will have consequences for the abundances of many chemically active trace gases in the atmosphere. Over the oceans and vegetated land surfaces, there can be significant fluxes of CO_2 both to and from the atmosphere. The flux of CO_2 from a variety of crops and forested regions has been measured for many years, using a variety of techniques. Some of these techniques, such as the dynamic or static chamber techniques, have been shown to have deficiencies (e.g., Baldocchi et al., 1986). Over agricultural surfaces, CO_2 flux has been measured by using a stability-corrected aerodynamic formulation (Verma and Rosenberg, 1976 and 1981). The eddy-correlation technique has been used to measure both

Table 1.11

Carbon Species Concentrations and Global Release Rates

Highest Priority Species	Critical Study Regions	Mixing Ratio Ranges in Each Region	Annual Release Rate	Comments
CH_4[1]	Natural wetlands	1.7–4 ppmv	100–200 Tg CH_4 yr^{-1}	
	Rice paddies	1.7–8 ppmv	60–170 Tg CH_4 yr^{-1}	
	Enteric fermentation (animals)		65–100 Tg CH_4 yr^{-1}	
	Biomass burning		50–100 Tg CH_4 yr^{-1}	
	Termites		10–100 Tg CH_4 yr^{-1}	
	Landfills		30–70 Tg CH_4 yr^{-1}	
	Oceans	1.7 ppmv	5–20 Tg CH_4 yr^{-1}	
	Freshwaters		1–25 Tg CH_4 yr^{-1}	
	Methane hydrate destabilization		0–100 (future) Tg CH_4 yr^{-1}	
	Coal mining		25–45 Tg CH_4 yr^{-1}	
	Gas drilling, venting, transmission		25–50 Tg CH_4 yr^{-1}	
CO	Biomass burning	Up to 1 ppmv	400–1600 Tg CO yr^{-1}	High concentrations in haze layers over Amazonia
	Continents	70 to 150 ppbv		
	Oceans	50 to 100 ppbv		
C_5H_8 (isoprene)[2]	Hardwood and tropical forests	1-50 ppbv C	350 Tg C yr^{-1}	Released daytime only; temperature dependent
$C_{10}H_{16}$ (terpenes)[2]	Coniferous forest	0.2-2 ppbv C	480 Tg C yr^{-1}	Temperature dependent
C_3H_6 (propene)	Rural continental	0.1-0.5 ppbv C		Ocean source very patchy. Concentrations up to a few ppb over ocean source regions
	Remote continental			
	Oceanic	a few ppbv		
C_2H_4 (ethene)	Rural continental	0.1 ppbv C		Ocean source very patchy. Concentrations up to a few ppb over ocean source regions
	Remote continental			
	Oceanic	a few ppbv		

Other Key Species:
CH_2O
CH_3CHO
$(CH_3)_2CO$
HCOOH
CH_3COOH
CH_3Cl

[1]Annual release rates from Cicerone and Oremland, 1988.

[2]Annual release rates from Zimmerman et al., 1978

the CO_2 emission from the floor of a deciduous forest (Baldocchi et al., 1986), and the CO_2 flux above the forest canopy (Verma et al., 1986). Eddy-correlation measurements of CO_2 flux from an aircraft have been reported by Desjardins et al. (1982 and 1989). Micrometeorological techniques have also been used to measure CO_2 flux over coastal ocean sites (Smith and Jones, 1985; Wesely et al., 1982a), but the values were significantly larger than those found by isotopic techniques (Broecker et al., 1986). The discrepancy has been discussed by Wesely (1986) and Smith and Jones (1986). Measurements of CO_2 concentrations in conjunction with other trace gases has sometimes been the basis for making estimates of the fluxes of these trace gases, as in the case of biomass burning (Crutzen et al., 1979; Seiler and Crutzen, 1980; Crutzen et al., 1985).

Methane

Fluxes of methane to the atmosphere have been measured or estimated from many known source types: wetlands (Svensson and Rosswall, 1984; Harriss and Sebacher, 1981; Sebacher et al., 1986), rice paddies (Cicerone and Shetter, 1981; Cicerone et al., 1983; Holzapfel-Pschorn and Seiler, 1986), animals (Crutzen et al., 1986), municipal solid waste (Bingemer and Crutzen, 1987), termites (Zimmerman et al., 1982; Seiler et al., 1984; Fraser et al., 1986b), biomass burning (Greenberg et al., 1984; Crutzen et al., 1985), and fossil fuel utilization (Ehhalt and Schmidt, 1978; Crutzen, 1987). Virtually all of the direct flux measurements have relied upon some variation of the enclosure technique. A notable feature of the results for wetland environments is the large range (approximately two orders of magnitude) of measured fluxes. For a variety of wetland sites in Alaska, Sebacher et al. (1986) found that the methane fluxes were significantly related to the water depth at each site. Large variations in methane fluxes have also been observed for termites, where the flux is strongly dependent upon the species of termite (e.g., Fraser et al., 1986b). In some cases fluxes of methane from the atmosphere into the soil have been measured (Keller et al., 1983; Seiler et al., 1984). More recently, fluxes of methane were measured with eddy-correlation techniques during the ABLE-3A experiment held in the Alaskan Arctic during July–August 1988. A fast-response methane sensor based upon the use of a helium-neon gas laser (Kolb et al., 1986) was used for flux measurements from an instrumented tower, while another fast-response sensor using a tunable diode laser (Sachse et al., 1987a,b) was used on board the NASA Electra to measure fluxes over large expanses of tundra.

In many cases the methane fluxes have an intrinsic interest, but usually the fluxes are extrapolated to the regional or global scale for the purpose of compiling global inventories of the sources and sinks of atmospheric methane. Over the past decade there have been several attempts to understand the global budget of methane in this way (Ehhalt and Schmidt, 1978; Sheppard et al., 1982; Khalil and Rasmussen, 1983; Seiler, 1984; Blake, 1984; Crutzen, 1987; Bingemer and Crutzen, 1987; Cicerone and Oremland, 1988). Given the very large uncertainties involved in extrapolating to the global scale from fluxes measured over areas of perhaps a few square meters, it is not surprising that there remain significant disagreements over the relative importance of various global sources of methane.

Carbon Monoxide

The global atmospheric budget of carbon monoxide, and its associated uncertainties, have been thoroughly discussed (Logan et al., 1981; WMO, 1986; Seiler and Conrad, 1987; Warneck, 1988). As much as 40% of the global source is attributed to anthropogenic activities, such as the burning of fossil fuels, agricultural burning, and the clearing of forests. One important feature of the CO budget is that at least 50% of the sources do not involve surface exchange of CO itself. Rather, the CO is produced in the atmosphere by oxidation of both biogenic and anthropogenic hydrocarbons. In addition, perhaps 40% of the global CO production occurs in tropical regions (Sachse et al., 1988; Andreae et al., 1988b).

Many of the terms in the global CO budget are not based upon direct measurement of CO fluxes. In fact, much of the information we have about the CO budget has been inferred from considerations of gas-phase chemistry (Logan et al., 1981), the measurement of CO emission factors from various types of combustion (Logan et al., 1981; Crutzen et al., 1985b; Greenberg et al., 1984; Andreae et al., 1988b), and estimates of the production and release of nonmethane hydrocarbons (Zimmerman et al., 1988). Since the tropics are thought to be such an important region for CO production, direct measurement of CO fluxes over large areas of the tropics would be very desirable. The first set of such measurements was made during the ABLE-2B flights over the Amazon Basin during the wet season (April–May) of 1987 using airborne eddy-correlation techniques.

The dominant sink mechanism for CO is oxidation to CO_2 by the hydroxyl radical, accounting for about 90% of the total. The remainder is thought to be lost by uptake in soils.

Nonmethane Hydrocarbons

It is now clear that the global flux of carbon into the atmosphere as nonmethane hydrocarbons (NMHCs) greatly exceeds the flux of carbon as CH_4. This flux is dominated by the release of biogenic NMHCs from vegetation, principally trees. The most important of these biogenic NMHCs are isoprene

(C_5H_8) and the monoterpenes ($C_{10}H_{16}$) such as α-pinene. In some tree species, such as pines and firs, the primary NMHCs emitted are the monoterpenes, while in other species (e.g., oaks and aspens) the primary NMHC product is isoprene. Some species, such as spruce and eucalyptus, produce both isoprene and monoterpenes (Rasmussen, 1981). Zimmerman et al. (1988) estimated that in the Amazon forest, isoprene accounted for approximately 20% of the gas-phase carbon of the NMHCs and that isoprene emissions were equivalent to approximately 2% of the net primary productivity of the forest (the net amount of carbon fixed during photosynthesis). The global annual release of isoprene from vegetation has been estimated as 450 Tg, with almost half of this total coming from tropical forests (Rasmussen and Khalil, 1988).

There have been relatively few attempts to measure fluxes of NMHCs into the atmosphere from the world's oceans. The available measurements indicate that the fluxes are small relative to those seen from land vegetation. Bonsang et al. (1988) have estimated an annual global release from the oceans to the atmosphere of 5.2 Tg (as carbon) of the C_2 to C_6 alkanes and alkenes.

The total annual emission into the atmosphere of biogenic NMHCs from the contiguous United States has been estimated as 31 Tg, with an uncertainty of a factor of three (Lamb et al., 1987a). By contrast, these authors estimate the anthropogenic NMHCs released from the U.S. in 1983 as 18 Tg. There is a strong seasonal and regional dependence of the biogenic emissions, with over half of the U.S. total occurring in the three summer months and approximately half the U.S. total coming from the southeastern and southwestern regions of the country (Lamb et al., 1987a). The total anthropogenic NMHC emissions in the U.S. are lower than the biogenic emissions; the anthropogenic releases occur principally from urban and industrial locations, which account for about 3% of the total land area, corresponding to areal fluxes about 20 times larger than those for biogenic source regions (Lamb et al., 1987a).

A variety of methods has been used to measure directly the fluxes of biogenic NMHCs. Some data are from measurements on live plants in a laboratory environment (Tingey, 1981), but most reported fluxes are from measurements made in the field. The laboratory measurements showed that higher temperatures increase the release of both isoprene and monoterpenes. Isoprene emissions occur only during daylight, with an increasing emission rate as the light intensity is increased. Monoterpene emissions do not vary with light intensity (Tingey, 1981). Field methods which have been used are an enclosure technique (Zimmerman, 1979a and b), a micrometeorological approach (Knoerr and Mowry, 1981; Lamb et al., 1985), and an atmospheric tracer technique (Lamb et al., 1986). The three methods give good agreement in measuring isoprene emission rates (Lamb et al., 1986).

The principal sink for atmospheric NMHCs is oxidation by the hydroxyl radical. Oxidation by species such as ozone and by the gaseous nitrate radical (NO_3) during the night does occur but constitutes a smaller sink (Winer et al., 1984). The reaction between isoprene and the hydroxyl radical is so rapid that during the daytime in the mixed layer over a tropical forest, isoprene controls the concentration of hydroxyl radicals (Jacob and Wofsy, 1988). Such oxidation of NMHCs leads to the formation of a variety of oxygenated substances such as aldehydes, organic acids, ketones, and organic nitrates (Lloyd et al., 1983; Kamens et al., 1982), which may undergo further rapid reactions to eventually produce carbon monoxide. Such oxidation of isoprene and other NMHCs over tropical forests has been observed to cause significant increases in the CO levels in the boundary layer (Gregory et al., 1986; Zimmerman et al., 1988). Oxidation of NMHCs can also lead to the formation of particulate matter.

Direct deposition of NMHCs to the surface may also occur, but it probably provides a relatively small sink compared to oxidation. The effectiveness of wet deposition for any particular species would depend upon its solubility in water as well as the pH of the precipitation droplets.

Organics

The species included in this category are those carbon-containing compounds (both vapor phase and particulate) other than CH_4, CO, the NMHCs, and the entirely man-made chlorofluorocarbons. Relatively little is known about this class of compounds in the atmosphere. For an extensive survey of the literature on the subject, the reader is referred to Duce et al. (1983). In this section we will concentrate on those areas where there have been recent advances in our understanding.

Formic acid and acetic acid are known to contribute to the acidity of precipitation, particularly in areas remote from significant anthropogenic influences (Keene and Galloway, 1988). Recent measurements by several investigators have greatly improved our understanding of the sources of these acids. Vapor phase concentrations of these acids typically range from less than 1 ppb to a few ppb (Dawson et al., 1980; Talbot et al., 1988; Andreae et al., 1988a). It is known that both acids are emitted from burning biomass and from motor vehicle exhausts (Talbot et al., 1988). Formic acid is produced by the oxidation of isoprene, while acetic acid is not (Jacob and Wofsy, 1988). It is likely that both acids are also emitted directly from vegetation (Graedel et al., 1986). Over the Amazon Basin, Andreae et al. (1988a) showed that over 98% of the total formic acid and over 99% of the total acetic acid are present in the gas phase, with

very small amounts present as aerosol. They found the highest concentrations of aerosol formate and acetate in haze layers associated with biomass burning. At a site in eastern Virginia, Talbot et al. (1988) also found both organic acids almost completely ($\geq$ 98%) in the gas phase, and that there were significant seasonal variations in the acid concentrations. The current knowledge of formic and acetic acids in the troposphere has recently been reviewed by Keene and Galloway (1988).

Research Needs

Based on the above discussion, we list in Tables 1.11, 1.12, and 1.13 the important nitrogen and ozone, sulfur, and hydrocarbon group species for which surface exchange needs to be studied. For each of the three groups the species are ranked into two priorities—highest priority species and other key species. The critical regions for study are listed for each species. Although not specified, it is obvious that measurements of temporal variations of the fluxes are essential, especially when surface exchange is related to biogenic processes.

Typical mixing ratio ranges in each region are listed as a guide for the required instrumental sensitivity and dynamic ranges. Also included are the expected ranges of surface flux or surface deposition velocity. In certain cases, surface resistance instead of deposition velocity is listed.

2 FLUX MEASUREMENT TECHNIQUES

M. L. Wesely, D. H. Lenschow, and O. T. Denmead

Several techniques have been developed to measure the rates of exchange of chemical species between the atmosphere and the surface. Principal among these are the aerodynamic methods, which quantify fluxes in air from tower and aircraft platforms, and nonaerodynamic methods, which usually involve a mass balance at or very near the surface. Each method has its advantages and disadvantages, as will be evident in the discussions that follow. None of the approaches is new; many represent extensions, modifications, or improvements of methods initially developed for estimating the fluxes of heat, momentum, and moisture important in meteorology and agriculture. To set the background for the detailed examination of modern applications of these methods to the surface exchange of chemical species, a brief historical review is appropriate.

Direct measurements of surface fluxes were apparently first attempted in order to estimate evaporation rates by using buckets and pans containing carefully monitored amounts of water exposed to ambient conditions near the surface. To this day, evaporation pans are standard in many meteorological observation systems. It is recognized, however, that these devices rarely, if ever, measure the evaporation rate characteristic of the surface in the vicinity of the pan and certainly do not measure characteristic evaporation when the surrounding surface is not wet. The term "potential evaporation" is used to describe the results obtained from a pan or from a thoroughly wetted surface. An important step toward measuring actual evaporation was taken with the development of the weighing lysimeter, which measures the rate of water loss from an isolated surface sample containing both soils and vegetation that are representative of the surrounding surface. Initial development took place in the 1930s (Hatfield, 1988). Weighing lysimeters now provide a standard of evaporation measurement in the agricultural scientific community.

Pans and lysimeters used for studies of the surface exchange of water have obvious counterparts in studies of trace gas and particle exchange: static and flow-through chambers used for measuring trace gas exhalation and surrogate surfaces used to investigate particle deposition. Despite the long history of development, it is clear that no technique that interferes with the processes that influence surface exchange can yield accurate measurements of the exchange from similar surfaces that are unaffected. For example, surrogate-surface measurements of deposition cannot easily be extended to nearby natural surfaces. Likewise, chamber techniques can distort the effects of atmospheric turbulence on exchange and the environmental conditions important in biological processes that affect exchange.

Aerodynamic methods for measuring exchange rates of trace chemical species are also founded on a long history of meteorological research. In general, modern methods rely on the measurement of either vertical gradients of time-averaged concentrations or on turbulent fluctuations of concentration. Gradient methods began with studies of wind near the surface and date back more than 70 years; Hellman (1915) and Johnson (1929) provide some early examples. Studies of near-surface atmospheric profiles were soon extended to temperature (e.g., Best, 1935). Eddy correlation, which involves sensing of turbulent fluctuations, was explored in the same period by workers such as Scrase (1930) but did not come to the forefront until electronic data-processing techniques became readily available in the 1960s.

The first eddy-correlation flux measurements from aircraft seem to be those reported by Bunker (1955). He estimated vertical air velocity by measuring vertical aircraft acceleration and horizontal airspeed fluctuations in conjunction with the aerodynamic characteristics of the airplane. Vertical velocity and airspeed fluctuations were used to compute an estimate of momentum flux, and sensible heat flux was measured by combining the output of a fine wire thermometer with the vertical velocity fluctuations. These early measurements, although somewhat crude by today's standards, established the usefulness of aircraft as platforms for turbulent flux measurements.

For the aerodynamic methods, it is not always clear that the flux measured in the air is the same as that at the surface. Rapid temporal changes in concentrations, large spatial inhomogeneities, fast chemical reactions, and a shallow boundary layer relative to the measurement height can all cause significant flux changes with height (i.e., flux divergence or convergence). As a result, it is usually necessary to

estimate or measure the spatial and temporal trends in local concentrations and wind field, the characteristic times of chemical reactions relative to vertical turbulent mixing, and the temporal and spatial variability of boundary-layer height.

It is often best to use more than one method to measure fluxes, to provide independent evaluations and to assess errors caused by some of problems mentioned above. The following three sections discuss some of the more promising methods now available, using towers, airplanes, and enclosures. Tower and aircraft techniques are discussed separately, because they tend to provide complementary spatial and temporal coverage and their technological requirements are somewhat different.

Tower-Based Flux Measurement Systems

Tower-based instrumentation systems for measuring air-surface exchange are well proven, convenient, and economical. Measurements at several meters above the surface can be used to quantify the average vertical exchange over several hundred square meters, along a path extending several hundred meters upwind and with a cross-wind breadth that increases with distance from the sampling tower. This "footprint" is not defined precisely, causing some difficulty when attempting to evaluate the air-surface exchange above a particular type of surface that borders other types nearby. The measured exchange rate incorporates fluxes to and from individual plants, surfaces beneath plant canopies, and individual portions of the surface such as leaves in a canopy. In summary, the sampling performed by tower-based flux measuring systems is representative of bulk surface properties over an area that depends on the height of the measurements.

Many tower-based methods of measuring the air-surface exchange of trace substances have been reviewed in recent publications concerned with dry deposition and surface energy balance (Kanemasu et al., 1979; Businger, 1986; Hicks, 1986; Hicks et al., 1986b). Much of the discussion here is based on the more detailed descriptions available in these publications and the references cited in them.

Traditional micrometeorological approaches are frequently used to measure air-surface exchange of trace chemicals. The methods addressed here fall most clearly into the category of micrometeorological techniques: eddy correlation, use of vertical gradients or profiles, and calculations of fluxes from variances of turbulent fluctuations. In some specific situations, however, alternatives may be required. Small-scale mass balances may be computed by integration of vertical profiles in horizontally homogeneous conditions, when vertical mixing is weak and the height of the upper boundary of the mechanically mixed layer in contact with the surface (the "lid" on vertical mixing) can be accurately estimated. Extremely stable atmospheric conditions or dense vegetative canopies can provide the opportunity for such mass balance studies. Carefully designed dual tracer methods provide another alternative. The sampling strategies must be precisely tailored to the physical conditions of the experiment. Similarly, special tracers can be employed. For example, ^{222}Rn or ^{220}Rn can, in special circumstances, provide information on exchange coefficients for nonreactive gases. Finally, numerical diffusion models can be used to obtain estimates of air-surface exchange with rather simple sampling strategies, if a small, isolated area of uniform emissions or uptake is well defined.

Inferential methods of surface exchange are designed to obtain operational estimates of dry deposition for which standard micrometeorological methods may be too difficult or too expensive to apply routinely. Inferential approaches are not considered here because they are not sufficiently direct; they are, in fact, based on parameterization experiments that employ more direct approaches. Surrogate surfaces may sometimes be appropriate for routine measurement of dry deposition but are not considered here because they do not measure fluxes that are directed upward.

Several requirements for micrometeorological measurements of vertical fluxes should be kept in mind. Substantial atmospheric nonstationary or horizontal advection should be avoided, or the effects should be taken into account by appropriate measurements and calculations. Flux divergences resulting from changes in the mean concentrations, entrainment through the top of the PBL, or mesoscale divergence may have to be evaluated, or at least detected, so that errors in micrometeorological flux estimates can be identified. For substances that undergo very rapid chemical reactions in air, measurements must be taken sufficiently close to the surface that the resulting changes of flux with height are small, if the intent is to evaluate exchange rates at the surface. This problem has arisen for measurement of fluxes of O_3, NO, and NO_2 and may be most easily addressed by use of both flux and profile measurements combined with modeling of chemical reactions. For many purposes, the complications of the chemistry can be avoided by measuring NO_z, which is a conserved parameter with respect to ozone oxidation and fast photochemistry.

Measurement of fluxes over nonuniform terrain requires especially careful analysis. In eddy correlation over sloping terrain, the proper distinction must be made between cross-streamline turbulent flux and mean transport. Established flux-gradient relationships may not be valid over nonuniform surfaces or complex topography. Likewise, the relationships between turbulent fluctuations and fluxes above nonuniform surfaces may be different from those over uniform surfaces.

3 STATUS OF CHEMICAL SENSORS FOR FLUX MEASUREMENTS

S. M. Anderson, A. C. Delany, F. C. Fehsenfeld, P. D. Goldan, C. E. Kolb, B. A. Ridley, and L. P. Steele

Typical mixing ratios for the priority atmospheric trace species discussed in Chapter 1 range from the parts per million to the parts per trillion level. Accurate measurement of such small chemical concentrations under field conditions, particularly of reactive species such as NH_3, NO_2, SO_2, H_2O_2, CH_2O, and O_3 is a major continuing challenge for atmospheric scientists.

The stringent requirements for chemical sensors utilized in the micrometeorological flux measurement techniques presented in Chapter 2 pose an even tougher challenge. The fast-response sensors (1 to 10 Hz) needed for tower- or aircraft-based eddy-correlation measurements or the high-precision concentration measurements needed for gradient profile studies (standard deviations of less than 1%) require sensitivity and/or accuracy that is, in general, beyond the current state of the art for measurements of most trace species concentrations. Although we do not explicitly discuss errors in flux measurement induced by nonlinear sensor response, they can also be significant in measuring means and fluctuations of trace species. Kristensen and Lenschow (1988) have examined the effects of nonlinear dynamic sensor response on measured means in a turbulent environment, but it appears that no one has considered its effects on flux measurements.

This chapter is a review of available chemical field measurement techniques for the trace species currently recognized as important in the evolving global atmosphere. This review also includes discussion of capabilities now undergoing development and testing that could be available for field work in the next year. Particular emphasis is placed on those technologies that seem most likely (either now or with further development) to satisfy the requirements of micrometeorological flux measurement procedures.

The following sections review contemporary techniques for trace species measurement. The first section summarizes methods for the oxidants, ozone and hydrogen peroxide, and members of the odd nitrogen family. The following section discusses measurement techniques for carbon monoxide, methane, and nonmethane hydrocarbons. The third section presents a summary of methods for detection of sulfur species, while the final section discusses particulate and aerosol detection.

Chemical Sensors for Oxidant and Odd Nitrogen

Because of the close links between the chemistry of the nonradical oxidants O_3 and H_2O_2, and odd nitrogen compounds, including NO, NO_2, NO_3, N_2O_5, HNO_3, HNO_2, PAN, and NH_3, it is frequently necessary to measure concentrations and/or fluxes of many species simultaneously in order to acquire sufficient insight into atmospheric processes. This section will review the status of detection technologies for these species and identify those species that can adequately resolve high-frequency fluctuations as required by the eddy-correlation flux measurement technique.

Ozone Detectors and Flux Divergence Measurements

In situ analyzers for ozone have been developed to the point where major field measurement programs are feasible without new technology. Two kinds of detecting mechanisms are widely used: chemiluminescence and ultraviolet photometry. Chemiluminescence, using nitric oxide as a reagent, has been used to make instruments with very fast response (bandwidths greater than 20 Hz), high sensitivity (below 0.1 ppbv), high specificity, and very low drift during operation. This method is preferred for many eddy-correlation measurements from both aircraft and towers.

It is of particular importance that the complete mechanism of nitric oxide–ozone chemiluminescence is well known, including all important kinetic rate constants. Thus, it is possible, in principle, to establish a calibration and measured operating parameters from these data. However, for practical reasons, chemiluminescence instruments are normally

calibrated against a photometric analyzer, which is an absolute standard.

Nitric oxide–ozone chemiluminescence has three limitations that, fortunately, do not significantly reduce its applicability. The first is a slight interference from water vapor, which is easily removed from eddy-flux measurements of ozone if simultaneous fast-response humidity measurements are made (Lenschow et al., 1981). The second limitation is the shot noise arising from discrete photons detected by the instrument. Since this noise is uncorrelated with measurements of vertical velocity, it does not bias estimates of the vertical flux by eddy correlation. Moreover, the current generation of instruments has sufficiently high sensitivity that shot noise does not contribute significantly to flux uncertainty. Shot noise does, however, contribute to both the power spectrum and variance of the ozone signal. Since at high frequency (in the inertial subrange region of atmospheric turbulence) the ozone spectrum is proportional to the $-5/3$ power of frequency, shot noise, which is white, tends to obscure the power spectrum for many typical atmospheric conditions. This limits the use of dissipation techniques for estimating ozone flux. Currently available sensitivities are probably adequate for using dissipation techniques within a few meters of the surface over land but are likely to be inadequate for measurements over water. If there is a strong need to employ dissipation techniques, the sensitivity of the nitric oxide–ozone analyzers can probably be increased to the point where power spectra over land could be measured to frequencies as high as 10 Hz. The third limitation is that the reagent nitric oxide is both toxic and difficult to remove from the vacuum pump exhaust. Thus, there is a potential for contaminating NO_y measurements in collocated surface experiments.

Chemiluminescence with ethylene or other olefins, such as cis-2-butene, is also used to measure ozone. This technique has the following disadvantages: (1) the reaction is slower and less sensitive than nitric oxide chemiluminescence, (2) the mechanism of light production is much slower, and (3) the temperature dependence of light emission is much greater. Suitably designed units can have a bandwidth as large as 1 Hz, making them suitable for tower-based eddy correlation at sampling heights of >5 m. An advantage is that the reagent olefin does not interfere with NO_y detection; however, it may be a factor if hydrocarbon measurements are collocated with the ozone sensor.

Ultraviolet photometry is the basis of practical, absolute ozone measurements generally made at the mercury 253.7 nm line. Commercial units have bandwidths of 0.03–0.05 Hz, while state-of-the-art research instruments have 1 Hz sampling (Profitt and McLaughlin, 1983; Profitt, 1985). Any of these devices can be used for gradient measurements, although the former typically have such a low precision (a few ppbv) that gradient applications are precluded in many common meteorological situations. The faster-responding versions are also suitable for tower eddy-correlation measurements. It should be noted that practical UV photometry is intrinsically a differential measurement. This property can and ought to be applied to gradient measurements. The major interference of this category of instrument is light scattering from ambient aerosols. While filters are employed by some investigators to remove particles, they can introduce additional uncertainties into the measurements.

In addition, tunable diode laser (TDL) IR absorption spectrometers and luminol chemiluminescence detectors are under development for in situ measurements. The availability of satisfactory techniques for in situ measurement lessens the requirement for development of TDL and luminol techniques for fast-response ozone measurements. Furthermore, TDL ozone instruments resemble those discussed for other species in later subsections. Therefore, they will not be discussed further here.

Remote sensors for tropospheric ozone concentration profiles are largely limited to IR and UV differential absorption lidar (DIAL) systems. Both types of systems have undergone extensive development in recent years, with the IR sensors offering somewhat greater spatial resolution at the expense of greatly reduced range. UV DIAL systems have been used to obtain ozone profile measurements at high resolution (50 m) through the entire troposphere. The exact performance of an ozone DIAL system is, however, more dependent on atmospheric conditions than are lidar wind profilers. Ozone concentration, temperature, aerosol distributions, and the spatial and temporal resolution requirements all affect the operational parameters selected for a particular measurement. This diversity of operational parameters, although providing an important means for optimizing the performance of the instrument for a particular measurement, nevertheless makes evaluating "typical" performance characteristics difficult.

Hydrogen Peroxide Detectors

A number of techniques are emerging to measure H_2O_2. However, these techniques do not yet have the sensitivity and/or response times needed to measure H_2O_2 flux by eddy-correlation techniques. Thus, experimental flux measurements are currently restricted to gradient and enclosure studies. Instrument comparisons have been carried out using many of the currently available detection methods, but the results from these studies are not yet available. The newly emerging techniques include: (1) the enzyme catalyzed dimerization of p-hydroxyphenyl acetic acid with continuous flow concurrent extraction (Lazrus et

al., 1986), (2) the same enzyme analytical technique with diffusion collection of the H_2O_2 (Hwang and Dasgupta, 1986; Dasgupta and Hwang, 1985; Dasgupta et al., 1986), (3) the enzyme analytical technique with nitric oxide pretitration of the ozone and subsequent collection of the H_2O_2 in an impinger (Tanner et al., 1986), (4) tunable diode laser absorption spectroscopy (Slemr et al., 1986) and (5) cryogenic trapping with peroxylate chemiluminescence detection (Jacob et al., 1986). Hartkamp and Backhausen (1987) review and evaluate several techniques for measurement of H_2O_2.

A highly selective, general-purpose detection method for many compounds is infrared TDL absorption spectrometry. A lead salt diode laser produces tunable radiation having a linewidth that is narrow compared to the Doppler-broadened vibrational-rotational lines for H_2O_2 and thus permits high selectivity. The laser repeatedly scans a single vibrational-rotational line; this serves to cancel background noise and allows measurements of absorbances lower than 10^{-5}. Absorption by H_2O_2 takes place within a White cell having a base path of 1.5 m and is operated at a pressure of 25 torr to minimize pressure broadening of individual lines. Present instrument configurations permit response times of 0.6 min. with detection limits of approximately 0.3 ppbv H_2O_2 with extended (>5 min.) signal averaging (c.f., Slemr et al., 1986).

The enzyme-supported detection of H_2O_2 is an innovative approach to detection of trace species in the atmosphere. Lazrus et al. (1986) report the detection of H_2O_2 and organic peroxides (ROOH) by first scrubbing them from the air into an aqueous solution using a continuous flow concurrent extraction. Next, 0.4 ml m^{-1} of scrubbing solution is drawn with the air sample into a glass coil; the velocity of the air spins the scrubbing solution to the walls, and the peroxides are dissolved into solution. The collection efficiency for H_2O_2 is estimated to be 100%; for methyl hydroperoxide and peroxyacetic acid, it is about 60%. The collection efficiency is lower for the organic hydroperoxides with higher molecular weights. The analytical chemistry for H_2O_2 is based on the reaction of peroxides with p-hydroxyphenylacetic acid (POPHA) in the presence of the enzyme peroxidase. This reaction forms the dimer of POPHA, which fluoresces with an emission wavelength of 420 nm when excited at 326 nm. Both H_2O_2 and short-chain organic hydroperoxides drive the analytical reaction.

Current instruments have detection limits of approximately 0.15 ppbv. The principal artifact identified is O_3, which may form some H_2O_2 in the solutions used in these instruments ($\geq$ 0.1 ppbv H_2O_2 equivalents). At present, the response time (10% to 90% for square wave analyte injection) is approximately 100 s.

Detectors for Odd Nitrogen Species

Whereas specific fast-response instruments have been developed and applied to micrometeorological flux determinations of O_3 (Pearson and Stedman, 1980; Lenschow et al., 1981; Gregory, 1987), instrument development for odd nitrogen has been directed towards maximizing sensitivity and specificity for ambient concentrations. With a few exceptions (Delany et al., 1986; Stedman, personal communication), little attention has been given to the provision of fast response for eddy-correlation applications. Consequently, most measurements of the surface exchange of odd nitrogen constituents have used enclosure, gradient, or budget techniques (Galbally and Roy, 1978; Johansson, 1984; Williams et al., 1987; Huebert and Robert, 1985). The species listed in Table 3.1 can be divided into three categories. The first includes those that hold promise for near-future eddy-correlation measurements using either towers or aircraft. The second includes those species for which monitoring techniques currently remain restricted to slower sampling methods. The third includes those species for which reliable techniques for even low sampling rates are not yet available, where details remain to be resolved before application to flux measurements, or where further instrument tests are needed.

The first category includes the TDL, LIF, and chemiluminescence instruments designed to measure NO. Many of these detectors have undergone measurement comparison tests successfully and have impressive sensitivities at low frequency (<1 Hz). Consequently, for locations where the mean NO concentrations are near or in excess of 0.1 ppbv, these instruments may be adequate for moderately fast-response ($\leq$5 Hz) flux measurement approaches. For example, the fast-response O_3 instrument of Pearson and Stedman (1980) utilizes the NO/O_3 chemiluminescence technique with NO as the reactant. Although it is much easier to generate high-reactant concentrations of NO than the reverse, where O_3 is used as the reactant, it should be possible to extend the frequency response of the chemiluminescence technique to 5–10 Hz. However, it must be emphasized that all but one of the NO or NO_2 instruments require an inlet system for aircraft or tower applications. The exception is the open cell, ambient pressure infrared diode laser technique, which is currently under development (Kolb et al., 1986; Anderson and Zahniser, 1988). Most of these instruments are large and are not "turn-key" operable. Clearly, adequate investigation (on-site and laboratory) of inlet lag times, surface effects, and true frequency response are necessary. Such tests would also be required for the direct NO_2 measurement instruments of Table 3.1 (i.e., TDL, luminol, and laser-induced fluorescence).

Table 3.1 Current Species Measurement Technologies — Oxidants and Odd Nitrogen Species

Species	Technique	Sample Method	Sampling Time (Range)	Detection Limit	Stability	Comments	References
O_3	Open path TDLAS[1]	Direct, no sampling	0.1 s	0.1 ppbv	To be evaluated	Under development	Kolb et al., 1986; Anderson and Zahniser, 1988
	Gas/liquid chemiluminescence (Eosin and relatives)[2]	Batch	0.1 s	0.3 ppbv	0.2 ppb if thermally controlled	Still under development, U. of Denver. A "conventional" luminol detector with a different reagent solution insensitive to NO_2 but sensitive to ozone. Lightweight, low power. No known interferences — also may be under development at Scintrex	Ray et al., 1986
	UV absorption	Continuous or batch	1–10 s	1–3 ppbv	1–3 ppb		Commercial versions available
	NO chemiluminescence[3]	Continuous	0.05 s	0.5 ppbv	> 0.5% at levels of 5 ppbv or higher	Slight interference from H_2O vapor, correctable from simultaneous measurements of moisture time series	Pearson and Stedman, 1980; Lenschow et al., 1981
	Ethylene chemiluminescence	Continuous	0.5 s	0.5 ppbv	1.3 ppb		Commercial version available
H_2O_2	Closed path TDLAS	Continuous	1 s – several minutes	~ 10 ppbv	To be supplied	Under development, no interferences, detection limits of ~ 1 ppb for 1 minute measurement times	Slemr et al., 1986

continued

Table 3.1 (Page 2)

Species	Technique	Sample Method	Sampling Time (Range)	Detection Limit	Stability	Comments	References
	Dual enzyme fluorimeter[4]	Batch	60 s	0.1 ppbv	0–1 ppb	Slow response — spaghetti machine	Lazrus et al., 1986
NO	Open path TDLAS[5]	Direct, no sampling	0.1 s	0.1 ppbv	To be verified	Under development	Kolb et al., 1986; Anderson and Zahniser, 1988
	NO/O_3 chemiluminescence	Continuous	1 s	10 pptv	1%	At 5 Hz, 50 pptv — sensitivity projected	Carrol et al., 1985; Drummond et al., 1983
	Two-photon laser/induced fluorescence[6]	Continuous	0.1–2000 s	150 pptv/1 s 5 pptv/30 s	± 2%	Improved sensitivity may be possible	Bradshaw et al., 1985, 1988
NO_2	Closed path TDLAS	Continuous	0.3 s – several minutes	0.3 ppbv	To be verified	Under development, no interferences	Schiff et al., 1983; Edwards and Ogram, 1986
	NO/O_3 chemiluminescence and photolysis[5]	Continuous	1 s	15–20 pptv	1%	Lag times or phase shift require measurement for higher-frequency operation	Kley and McFarland, 1980
	Photofragmentation/two-photon laser-induced fluorescence[7]	Continuous	5–2000 s	250–pptv/1 s	± 2%	Requires subtraction of ambient NO mixing ratio; large sensitivity improvements may be possible	Bradshaw et al., 1988
	Luminol	Continuous	0.3 s	1 pptv	± 2%	PAN and O_3 interferences are possible; commercial version available from Scintrex-Unisearch	Wendel et al., 1983

continued

Table 3.1 (Page 3)

Species	Technique	Sample Method	Sampling Time (Range)	Detection Limit	Stability	Comments	References
	Long path absorption	Direct, no sampling	1 s–1 hour	Untested	Variable	Sensitivity and stability dependent on atmospheric conditions. Detection limit of 0.08 ppbv for measurement time of ~ 20 min.	Platt and Perner, 1980
PAN	Air carrier gas, GC with luminol detection	Continuous or batch	1 sample/30 s is as fast as has been demonstrated	10 pptv	Not applicable to GC	No known interferences in GC method. No compressed gases required. Nonlinear calibration necessary at low end. Low power and weight requirements. Still under development, U. of Denver/Scintrex	Burkhardt et al., 1988
	Electron capture gas chromatography[8]	Continuous or batch	.02 Hz	40 pptv	4% (precision)		Penkett and Brice, 1986
HNO_3	Closed path TDLAS	Continuous	1 s to several minutes	To be verified	To be verified	Under development, no interferences	Schiff et al., 1983
	Tungstic acid	Continuous	15 min.	0.1 ppbv	10%	Potential interference from organic nitrates	Braman et al., 1982
	HNO_3 by nylon or impregnated filter[9]	Batch	30 min. (direct trade between speed and sensitivity)	0.1 ppbv	No drift but filter zero is a problem	Ion chromatographic analysis, very slow; only possible for gradients. Problem with nylon formulations changing so the NO_2 interferes	Huebert and Lazrus, 1980

continued

Table 3.1 (Page 4)

Species	Technique	Sample Method	Sampling Time (Range)	Detection Limit	Stability	Comments	References
NO_3	Long path absorption	Direct, no sampling	1 s	Untested	Variable	Sensitivity and stability dependent on atmospheric conditions. Detection limit of ~ 1 pptv for times of ~ 20 min.	Platt et al., 1984
HONO	Photofragmentation two-photon laser-induced fluorescence[10]	Continuous	60–2000 s	80 pptv/60 s	± 15%		Rodgers and Davis, 1988
	Long path absorption	Direct, no sampling	1 s – 1 hour	Untested	Variable	Sensitivity and stability dependent on atmospheric conditions. Detection limit of 0.02 ppbv for measurement times of ~ 20 min.	Platt and Perner, 1980
NO_y	Hot molybdenum[11]	Continuous	0.01–1 s	(0.01 ppbv for 1 s sample)	10%	See Fehsenfeld et al., 1987. NO_y technique intercomparisons.	Dickerson et al., 1984
	Master blaster + luminol[12]	Continuous	10 s	50 pptv	< 25 ppt	Compared against master blaster + ($NO + O_3$) chemiluminescence.	Bakwin et al., 1988
	Master blaster + converter Au/CO[13]	Continuous	1 s	10 pptv	1%	Lag times or phase shift require measurement for higher frequency operation.	Fahey et al., 1985
	Chemical conversion/two-photon laser-induced fluorescence[8]	Continuous	5–2000 s 5 pptv	150 pptv/1 s 5 pptv/30 s	± 2%		Bradshaw et al., 1985, 1988

continued

Table 3.1 (Page 5)

Species	Technique	Sample Method	Sampling Time (Range)	Detection Limit	Stability	Comments	References
NH_3	Open path TDLAS	Direct, no sampling	0.1 s	To be evaluated	To be evaluated	Under development	Kolb et al., 1986; Anderson and Zahniser, 1988
	Closed path TDLAS	Continuous	1 s – several minutes	To be evaluated	To be evaluated	Under development	MacKay and Schiff, 1984
	Tungstic acid denuder[14]	Continuous	15 min.	0.1 ppbv	10%		Braman et al., 1982
	MO_3 denuder[15]	Continuous	15 min.	0.1 ppbv	10%		Langford et al., 1988
	Wet trapping[16]	Batch	1–2 hours	0.5 ppbv	n/a		Denmead et al., 1976; Denmead et al., 1977
	Dry trapping[17]	Batch	1–2 hours	0.5 ppbv	n/a		Ferm, 1979
	VUV-photo-fragmentation/ laser-induced fluorescence[18]	Continuous	60–2000 s	15 pptv/60 s	± 10%		Stickel et al., 1988
	Condensation	Batch	10–15 min.	50 pptv		Sampling time dependent on ambient water vapor	Dawson and Farmer, 1984

END NOTES — Table 3.1

1. *Tunable Diode Laser Description*: The attractiveness of tunable diode laser absorption spectroscopy (TDLAS) for atmospheric trace gas sensing stems from the broad wavelength coverage available (3–30 μm for sub-77K lasers), enabling virtually any IR-active species to be detected. Both types of instruments listed in Table 3.1 couple TDL light sources with a multipass absorption cell. In the closed path version, ambient air is drawn through a sampling system into a reduced pressure absorption cell to exploit the Doppler-limited spectral resolution afforded by the inherently narrow laser line widths. In the open path system, the multipass mirror set is positioned in the free air to maximize frequency response and sample integrity and relies on the rapid tunability of TDLs to relieve spectral congestion. The fundamental limits set by the minimum detectable fractional absorption ($\sim 10^{-5}$), molecular IR line strengths, and useful absorption path lengths ($\sim$ 100 m) can provide detection limits in the sub-ppbv range.

   From a practical viewpoint, the relative complexity of the optical train required for laser mode separation and the need to operate these lasers below 77K has reduced the utility of TDL systems in fixed environments. Extension of recent developments in higher temperature, single mode lasers to a broader wavelength range is improving this situation considerably. Coupled with further improvements in detectable fractional absorption demonstrated using RF modulation (10^{-6} - 10^{-7}), in path lengths using new types of multipass cells ($\sim$ 1 km), and the capability for simultaneous multilaser/multispecies instruments, TDL systems will probably become powerful tools for atmospheric trace gas measurement.

2. A system in which an air compressor provides both carrier gas (through an $FeSO_4$ trap) and sample (when the scrubber is bypassed) to a short column terminating in a standard luminol detector. Sensitivity and nonlinearity are a function of additives to the luminol solution and will remain the subject of discussions among users.

3. Ambient air is mixed with 5% to 10% nitric oxide (99% cp grade) and the resulting chemiluminescence is measured with a cooled, red-sensitive photomultiplier. The method is sensitive, fast, and quite specific. The only known interference is a slight quenching from water vapor, which is readily corrected if moisture is measured simultaneously. If O_3 flux is to be measured, the preferred correction is with the moisture flux.

4. Gas phase H_20_2 is absorbed in water and determined by derivitration/fluorimetry. Enzymatic reactions are used to distinguish H_2O_2 from organic peroxides.

5. Instruments all use well-known chemiluminescent reaction between NO and O_3. Specifications given for research versions where care taken for flow, temperature, humidity, and ozone stabilization. NO_2 is detected as NO by ultraviolet photolysis ($\lambda > 320$ nm) of NO_2 (efficiency $\sim$ 50%).

6. *Laser-Induced Fluorescence Techniques*: Laser-induced fluorescence provides a highly sensitive and spectroscopically selective method for measurement of a number of species of atmospheric interest. Early instruments exploiting this technique employed single photon and were therefore limited to the detection of strongly fluorescent molecules such as NO, SO_2, or OH or to detection of weakly fluorescent molecules at high concentration, such as NO_2. Recent efforts have extended the applicability of the technique through the use of laser photofragmentation and two-photon, background-free, fluorescence excitation schemes.

   Although detectable by single-photon excitation, current NO laser-induced fluorescence sensors employ a two-photon excitation approach. In this method, NO molecules are first excited into their lowest-lying electronically excited state by absorption of 226 nm laser photon. Subsequently a fraction of these excited NO molecules absorb a second laser photon at $\sim$ 1080 nm and are excited into a higher electronically excited state by absorption of a second laser photon at $\sim$ 1080 nm. The resulting fluorescence, centered at $\sim$ 185 nm, is blue-shifted relative to both pumping wavelengths. In conjunction with appropriate blocking filters and photomultiplier tubes, this blue-shifted fluorescence can be almost entirely discriminated from scattered laser light and emission from other atmospheric species and thereby provides a background-free signal for detection of NO.

7. Current LIF sensors measure NO_2, NO_n, and NO_y by conversion to NO followed by detection using the two-photon, laser-induced techniques. In the case of NO_2 this conversion is accomplished by laser photolysis of ambient NO by the output of a 351 nm XeF excimer laser. Since the NO_2 photolytic efficiency can approach unity, total NO_n can be readily detected by this approach. In the case of NO_y, detection of NO follows conversion in a catalytic reactor.

8. Uses a low temperature detector (40–50°C), ^3H electron capture gas chromatograph, ~20 cm^3 (STP) sample collected cryogenically, elution times typically 5 to 6 minutes. (Detection limit can be changed by varying the collection time.)

9. Teflon filter keeps particulate NO_3^- out, but there is some volatilization. The same tailend analysis works for a denuder or annular denuder, which may be better at distinguishing vapor from particulate NO_3^-.

10. Like NO_2, HONO is detected by near-ultraviolet laser photolysis. In the case of HONO, however, the detectable photofragment is OH, which is detected by a single-photon, laser-induced fluorescence.

11. Metallic molybdenum at ~ 400°C has been demonstrated to be a quantitative and fast NO_y converter with no NH_3 conversion. The basic reaction is of the form $NO_y + Mo \rightarrow O_n + NO$. Time response of < 1 s for NO_2 and PAN is relatively straightforward. Fast time response for HNO_3 in a system which is stable, drift free, and easily calibrated and zeroed has yet to be developed. (Research is under way at the U. of Denver, but outcome is uncertain.) Major caveat is that the system must be used carefully because molybdenum oxide powder ablates from the converter.

12. A gold tube converter master blaster (Fahey, et al., 1985) with H_2 reductant converts NO_y to NO. The NO is reacted in a quartz tube with O_3 to make NO_2, which is detected using a Luminol-3 luminol instrument. The instrument is zeroed by combining the O_3 and sample air just before the detector, bypassing the quartz tube. The O_3 level is kept constant at ~ 1 ppmv, which eliminates the nonlinearity of the luminox machine. The unit is lightweight and uses little power.

13. Total odd nitrogen reduced to NO with 95% to 100% conversion using gold/CO converter operated at 300 to 325°C.

14. *Tungstic Acid Denuder.* NH_3 is absorbed on the surface of a denuder tube coated with tungstic acid. The NH_3 is desorbed and subsequently converted to NO, which is detected by chemiluminescence. HNO_3 is also collected and desorbed as NO. The NH_3 and HNO_3 are separated by temperature programming desorption or by sequencing the NH_3 conversion process.

15. *Molybdenum Oxide Denuder.* NH_3 is absorbed on the surface of an oxidized (VI oxide) molybdenum tube. After absorption sequence, the tube is heated with a flow of zero air passing through the tube. The NH_3 is partially desorbed (~ 30%) as NO. The NO is detected by a chemiluminescence detector.

16. Air is drawn through trap containing glass beads impregnated with 1% phosphoric acid. Flow meters are used to monitor flow rate or volume of air through traps. Authors used flow rate of 10 ℓ/min. After air sampling, NH_4^+ is eluted from tap with distilled water and measured with an NH_3-specific ion electrode.

17. Air is drawn through glass tube coated with oxalic acid. Acid later washed out and NH_4^+ determined with NH_3-specific ion electrode.

18. NH_3 is currently measured by sequential photofragmentation of NH_3 and its photo-products, first to form NH_2 and then to form metastable $NH(^1b)$, by the 193 nm output of an ArF excimer laser. After an appropriate time delay (1 to 5 μs), the NH(b) is further excited by absorption of an ~ 450 nm laser photon that results in intense blue-shifted fluorescence at 326 nm. This fluorescence, although blue-shifted relative to the 450 nm probe wavelength, is not completely background free due to residual fluorescence resulting from the interaction of the 193 nm photolysis beam with the chamber walls. This residual background is, however, very small due to the substantial time delay between the passage of the photolysis and probe laser beams.

The first category also includes instruments for NO_2 and total reactive odd nitrogen (NO_y) based on the detection of NO resulting from the chemical or physical reduction of these species. This conversion can result from photolysis (in the case of NO_2) or chemical conversion on hot surfaces (for both NO_2 and NO_y). These techniques, with their high sensitivities, hold promise for fast-response flux determinations, but laboratory assessments of the overall instrument frequency response are also required. For example, for frequencies larger than about 1–2 Hz, inlet, converter, and reaction memory effects need to be investigated to determine possible filtering of the response. Clearly, the higher mean concentrations of NO_y present a distinct advantage for possible high-frequency measurements. However, as outlined elsewhere in this report, NO_y flux determinations without concurrent flux measurements of other family members are often not particularly useful.

The second category includes instrumentation for NO_2, PAN, HNO_3, NH_4^+, NO_3^-, and HONO. Here, the precision of current measurement techniques is sufficient for gradient methods and certainly for budget or enclosure methods. Instrument comparisons have been conducted for most of these species. There are also long-path absorption methods available for NO_2 and for nighttime NO_3 and HONO (Platt et al., 1984; Platt and Perner, 1980). However, their application to surface exchange measurements needs to be investigated.

It is more difficult to categorize current instrumentation for NH_3 and HNO_3. Techniques for both species are available, but the results of instrument comparison studies for HNO_3 (and planned for NH_3) are not yet generally available. The reluctance of the community to accept these methods is mainly associated with sampling difficulties rather than detection. These species are notoriously difficult to transport unperturbed through inlets, and losses through sample handling can be severe. These factors can also make calibration difficult. A novel alternative for NH_3, involving a vane-mounted sampler that measures fluxes directly (with some surface-layer structure assumptions), may prove useful (Leuning et al., 1985).

The third category is obvious from a cursory examination of Table 3.1. For example, no measurement techniques are currently available for N_2O_5, HO_2NO_2, or many organic nitrates (other than PAN or PPN).

In summary, there are a variety of measurement schemes for odd nitrogen species, many of which are based on the sensitive detection of NO (O_3/NO chemiluminescence or two-photon laser induced fluorescence) or NO_2 (luminol). Other species of NO_y are detected either by heterogeneous chemical conversion or by photolytic conversion. The exceptions to this general detection scheme are the TDL and the filterpack methods. All of these provide detection limits in the low pptv range, although the integration times required to attain this level range from one second to tens of minutes for the chemiluminescence, TDL, LIF, and filter pack methods, in roughly that order. Most of these instruments have been developed for high sensitivity with little consideration of frequency response. Moreover, the difficulty in sampling "sticky" gases like HNO_3, HONO, and NH_3 through an inlet system limits the time response of many instruments. Open path absorption methods may alleviate many of these problems and provide higher frequency response for such species.

Carbon Monoxide, Methane, and Nonmethane Hydrocarbon Sensors

Most of our knowledge about the atmospheric distributions of the carbon species CO, CH_4, and nonmethane hydrocarbons (NMHC) has been obtained by gas chromatographic analyses using flame ionization detection. This detection technique can be used with continuous sampling systems, but it is most often used for grab samples, often processed a considerable time after sampling. Quite recently, however, tunable laser techniques have been developed that allow real-time and fast-response measurements of CO and CH_4. These techniques are discussed in further detail below and summarized in Table 3.2.

Fast-Response Sensors for CO and CH_4

Gas sensors using semiconductor TDLs have the potential for making measurements of many important atmospheric gas species. The wide applicability of TDL-based sensors is due to the availability of lead-salt TDLs, which may be composition tuned to operate near a particular wavelength in the spectral region between 3 and 30 μm, where most atmospheric species have absorption bands. Other semiconductor laser sources fabricated from III-V compounds are also available in the near-infrared spectral region. The ease of wavelength modulation of TDLs (simply by modulating the laser injection current) enables highly sensitive differential absorption ($1{:}10^4$ to $1{:}10^5$) detection of many gas species.

A fast-response TDL sensor has been developed to measure CO from an aircraft (Sachse et al., 1987a; 1987b; 1988). A TDL lasing in the 4.7 μm spectral region is used to detect ambient CO in a White cell containing a 12.5 m absorption path. Instrument response time depends on the air sampling rate; consequently, a low-volume White cell and a vacuum pump with a high pumping speed are important factors in achieving the rapid response required for airborne eddy-flux measurements. A high performance air sampling system has been developed using a venturi air jet ejector vacuum pump that is driven by bleed air from an aircraft engine compressor (Sachse et al.,

1987b). This TDL sensor has achieved a 1/e response time of 70 ms using a 1.5 liter White cell volume and a 2,500 ℓ min^{-1} pumping speed (at 100 torr). Substantial reductions (by a factor of three or more) in White cell volume are readily achievable and will result in further improvements in the time response of TDL gas sensors.

Recent modifications of this instrument have enabled it to make simultaneous, fast-response measurements of CO and CH_4 during the ABLE-3A expedition to Alaska. Methane detection is accomplished using an additional TDL lasing in the 7.6 μm spectral region. By beam combining the radiation from the 4.7 μm and 7.6 μm TDLs using a dichromic beam splitter, the two laser beams follow a common path through the White cell, permitting simultaneous differential absorption measurement of CO and CH_4. A "two-color" detector consisting of a sandwich structure of InSb on HgCdTe enables independent detection of the differential absorption signals occurring at the two wavelengths.

While TDLs are extremely versatile, they require careful handling and significant talent to operate. Furthermore, they consume considerable power, especially if the laser must operate at below 77 K (liquid nitrogen temperature). Many of these problems can be avoided if a gas laser can be substituted for the TDL.

Rare gas laser infrared absorption detectors rely on accidental close coincidences between an atomic line of the lasing medium and an appropriate molecular transition. Such coincidences occur for HeNe and CH_4 (2,947.9 cm^{-1}), and HeXe and N_2O (2,467.4 cm^{-1}), among others. Zeeman splitting of the laser gain line over a portion of the plasma column provides three possible emission wavelengths, which are scanned by modulating the cavity length to sense differential absorption (Kolb et al., 1986; McManus et al., 1989). Depending on the nature of the laser power control loop, the instruments can be configured to detect either absolute concentration or, with increased sensitivity, small concentration fluctuations as needed for eddy correlation. The lasers are small and rugged, and can be coupled to either open- or closed-path multipass absorption cells. Detection levels are similar to those obtainable with TDL systems, since similar differential absorption signal processing is involved.

A unique fast-response method that has been used for CH_4 chamber flux measurements utilizes a gas-filter-correlation IR absorption analyzer coupled to either a closed or an open sampling chamber (Sebacher, 1978; Sebacher and Harriss, 1982; Harriss et al., 1982; Harriss et al., 1985). This technique provides continuous sampling and analysis of the air in the chamber, with high precision ($\pm$10 ppb for CH_4) and a response time of 1 s, enabling CH_4 fluxes as small as 10^{-12} kg CH_4 m^{-2} s^{-1} to be measured in a 15-minute sampling and analysis period. The continuous measurement of CH_4 in the chamber allows variations in the flux rate during the sampling period to be readily identified. The rapid response of the technique, combined with the chamber design, allow any disturbances to natural systems during flux measurements to be kept to a minimum.

Slow-Response Methods for Hydrocarbons

Currently, fast response sensors for NMHCs are not available. Measurement of species such as ethylene, propene, isoprene, and the monoterpenes requires collection of discrete samples of sufficient volume to permit quantification by gas chromatography. Consequently, enclosure and tower (gradient) procedures are applicable to the measurement of NMHC fluxes but eddy-correlation methods currently are not. Table 1.11 lists the ranges for ambient hydrocarbon concentrations observed in various environments. Concentrations of many NMHCs in clean oceanic air masses may be as low as 0.1 ppbv (Bonsang et al., 1988), which is close to the detection limit of current methods. In contrast, ambient isoprene concentrations, which fall in the ppbv range in the vicinity of hardwood forests on hot summer afternoons, can be measured with certainty.

Grab-sample methods for NMHC and CH_4 measurements have existed for several years (Steele et al., 1987; Sexton and Westberg, 1979; Roberts et al., 1983; Rudolph et al., 1981; Singh et al., 1985). Whole-air samples are collected in either glass or electropolished stainless steel containers. Analysis is by gas chromatography (GC) with flame-ionization detection. Preconcentration by cryogenic trapping of the NMHC is normally necessary prior to injection into the chromatograph. The sample collection method readily allows for sampling at different heights on a tower or aircraft. Tethered balloon sampling can be accomplished by collection into teflon bags (Zimmerman et al., 1988).

Techniques for carbonyl species sampling include high-pressure liquid chromatography (HPLC) of samples collected on impregnated cartridges (Kuntz et al., 1980) and cryogenic collection into glass loops followed by analysis with a flame ionization detector (FID)-equipped gas chromatograph (Snider and Dawson, 1985). The cartridge method collects carbonyl compounds by passing air through silica cartridges impregnated with 2,4-dinitrophenylhydrazone. Samples are then eluted from the cartridges and analyzed by high-pressure liquid chromatography (HPLC). The GC technique provides measurement of many C_2–C_5 carbonyls with detection limits in the lower ppt range. Both of these methods are appropriate for measurements on towers as well as aircraft.

Several methods exist or are under development to measure organic acids. These include condensation sampling (Farmer and Dawson, 1982), a mist chamber (Talbot et al., 1988), denuder tubes (Norton,

1986), and impregnated filters. Results from an intercomparison of these methods during June 1986 showed agreement between all systems except for the impregnated filters (Keene et al., 1989). Most of the existing data have been collected by the use of the condensation method—cooling a highly polished, clean surface below the dew point temperature so that a film of water collects on the surface. Highly soluble gases are collected with essentially unit efficiency. Ion chromatography or ion exclusion chromatography provides measurement of organic acid concentrations in the condensate. These concentrations are then used to calculate gas-phase levels of the acids. Tower and aircraft measurements are possible with all current systems with the exception of those that use the condensation technique.

Sulfur Species Chemical Sensors

As discussed in Chapter 1, the mixing ratios of sulfur species in the atmosphere, in almost all regions free of industrial pollution, are < 1 ppbv. The measurement of such low concentrations of reactive and labile sulfur compounds of interest, such as H_2S, CH_3SH, SO_2, and CH_3SCH_3 (DMS), and even the more stable species COS and CS_2, has been a serious challenge and the most significant motivation for the development of sulfur-specific detectors. Those detectors currently available or known to be under development are listed in Table 3.3, together with the sulfur species for which they are applicable, estimated sensitivities, and sampling-related information.

Detectors Sensitive to a Variety of Sulfur Compounds

The oldest (~20 years) of the listed detection techniques is the flame photometric detector, or FPD. Its sensitivity to sulfur compounds relies on thermal decomposition of the compounds in an oxy-hydrogen flame with the subsequent occasional formation of an electronically excited S_2 molecule that can radiate in the near UV. The detection of photons from those molecules that escape collisional de-excitation is the signal-producing mechanism. Since the FPD relies upon the formation of an S_2 molecule, its sulfur response is inherently nonlinear. Recently, a number of workers (D'Ottavio et al., 1981; Goldan et al., 1987) have lowered the detection limit of the FPD and circumvented this nonlinearity by intentionally adding some convenient volatile sulfur species to the flame combustion gases. If the detected sulfur species concentrations are small compared to the added species (commonly SF_6), the differential response is quasi-linear.

A number of chemiluminescent sulfur detectors that have recently been developed are also included in Table 3.3. These depend upon the reaction of a specific class of sulfur compounds with a gas-phase chemical reagent to produce electronically or vibrationally excited species whose subsequent radiation can serve as a detection mechanism. Spurlin and Yeung (1982) claim a detection limit of 3 ppbv for H_2S by using its reaction with ClO_2. Kelly et al. (1983) observed the chemiluminescent reaction of a number of sulfur-bearing compounds with O_3 and showed a detection of DMS in the low ppbv range, with higher sensitivity for CH_3SH and much lower sensitivity for H_2S. Perhaps the most promising of the chemiluminescent detection techniques is that described by Nelson et al. (1983), in which sulfur compounds react with F_2. Recent work with this type of detector shows promise of achieving detection limits of ~1 pg S per sample, somewhat lower than that achieved with an SF_6 doped FPD. Since this response to different sulfur compounds varies a great deal (negligible response to SO_2, COS, H_2S, and CS_2 was reported), its use in the measurement of sulfur fluxes in the atmosphere appears limited.

A recent development in sulfur gas detection is the use of an electron capture detector (ECD); (Johnson and Lovelock, 1988). Sulfur-bearing compounds may be converted to SF_6 at moderate temperatures (~ 200°C) by reacting them with AgF_2. Since the resulting SF_6 has a large electron capture cross section, it may be readily detected with an ECD, thereby taking advantage of that detector's extremely high sensitivity. The AgF_2 is replenished by supplying a small amount of fluorine gas to the sample stream. Since the ECD is also sensitive to F_2, the excess F_2 must be removed by reacting it with H_2 on a hot palladium catalyst. Although this technique is in its infancy, the procedure is fraught with technical difficulties, and its application is likely to be limited to skilled practitioners, it offers great promise. The method should yield a detection limit some hundred times lower than even the doped FPD.

Application to Total Sulfur Measurements

Since both the FPD- and ECD-based detection schemes described above are sensitive to all sulfur-bearing compounds, either may be used as a total sulfur detector, as well as in systems where the sulfur compounds are speciated. The undoped FPD is capable of detecting changes in sulfur flow of approximately 3×10^{11} molecules s^{-1} and the doped FPD of approximately 4×10^{10} molecules s^{-1} under optimum circumstances. Since typical sample flows may be made as high as 0.2 ℓ min^{-1} STP, these correspond to mixing ratios of approximately 3 ppbv and 0.5 ppbv, respectively. Thus, the FPD has sufficient sensitivity for total sulfur measurements, at least in somewhat polluted environments, and much of the deposition flux work to date has utilized an FPD-based system. By minimizing sample throughput times, response times of the order of a second (or slightly less) can be achieved, but the FPD remains inherently noisy, even for levels of sulfur gases (predominantly SO_2)

found in moderately polluted air. Pressure fluctuations affecting the flame and collisional quenching by other minor atmospheric species (such as CO_2 and H_2O) present operational problems that were difficult to overcome in early applications of FPD techniques in eddy-flux studies, and which remain the sources of continuing concern. FPD detectors optimized for fast response have been utilized for eddy-correlation measurements of total sulfur deposition in many studies in moderately polluted environments (e.g., Hicks et al., 1986a).

The inherently greater sensitivity of an ECD-based system holds greater promise in that regard. Its detection limit, estimated to fall in the range of 5×10^8 to 10^9 molecules s^{-1}, coupled with a sample flow rate of $\sim$ 20 cm^3 min^{-1}, results in a detection limit of 50 to 100 pptv. Detector time constants < 1 s can be achieved by increasing the sample flow rate and decreasing the detector volume with some loss of sensitivity. Since such a system would be compatible with the requirements of micrometeorological techniques, its development would appear highly desirable. Using either an FPD or ECD detector-based system for the measurement of volatile sulfur gas fluxes requires, of course, the removal of $SO_4^=$ aerosols prior to analysis and dealing with the problems associated with different sensitivities for different sulfur compounds.

Species-Specific Detectors — Fast Response

Table 3.3 also lists several laser and nonlaser spectral techniques that can be used to monitor specific sulfur compounds with detection limits expected to fall in the 0.2 to 1 ppbv range. Of these, two new techniques show promise for the sensitive, rapid, real-time detection necessary for eddy-correlation flux measurements. The first of these uses differential optical absorption of TDL radiation in either an open, atmospheric pressure multipass region (Kolb et al., 1986; Anderson and Zahniser, 1988), or a closed, lower pressure, multipass absorption cell (Edwards et al., 1984; Edwards and Orgram, 1986). This technique, which is expected to have a detection limit near 1 ppbv for SO_2, is currently under development for eddy-correlation flux measurements.

The second approach is the vacuum UV flash photolysis/laser-induced fluorescence (VUV-FP/LIF) technique. In this method, a parent sulfur species (SO_2, H_2S, or CS_2) is photodissociated by 193 nm photons from a pulsed ArF excimer laser. The resulting molecular fragments (SO, HS, or CS) are then detected by induced fluorescence from a tunable dye laser. This innovative technique is estimated to be capable of a detection limit of $\sim$ 150 pptv but is more equipment intensive than the TDL approach.

Both of these techniques exploit the specificity of spectral detection, along with the high sensitivity and temporal resolution often possible with sophisticated laser techniques. It should be recognized, however, that lasers are expensive and frequently difficult to incorporate in field instrumentation, and usually require advanced skills to operate successfully.

Species-Specific Detectors — Slow Response

No species-specific detectors with sufficient sensitivity to measure ambient levels of biogenically produced sulfur compounds on time scales suitable for eddy-correlation flux measurements are currently available. The measurement of such compounds (most notably DMS) requires some type of sample concentration followed by analysis, with the possible exception of the ECD-based scheme described above. If the concentration step is species specific, it may be followed directly by detection. More generally, however, the concentration step is followed by species separation by some type of chromatography with subsequent individual species quantification. Such batch or grab sample processing techniques typically have time scales ranging from several minutes to several tens of minutes. Thus, flux measurements for these species will be restricted to gradient techniques.

Currently available analysis techniques of this type are also summarized in Table 3.3. The sample concentration techniques utilized in the measurements referred to are summarized in Table 3.4. Some of these sample concentration techniques are amenable to subsequent species-specific detection and some only to classes of sulfur compounds as noted in the table. Those techniques that utilize liquid extraction are generally amenable only to ion chromatographic analysis and lead to much higher ($\sim 10^3$) detection limits. The flash vaporization technique results in a nonspecific "total sulfur" sample.

Table 3.2 Current Species Measurement Technologies — Carbon Monoxide, Methane, Nonmethane Hydrocarbons, and Organics

Species	Technique	Sampling Method	Sampling Time (Range)	Detection Limit	Stability	Comments	References
CO	Closed path laser differential absorption	Continuous	.05 s to minutes	10 ppbv	~ 1%	Flight demonstrated	Sachse et al., 1987a,b; Sachse et al., 1988
	Mercuric oxide detector after GC separation	Batch	Seconds to minutes	~ 1 ppbv	Not applicable	Commercially available	
CH_4	Diode laser differential absorption	Continuous or direct	.05 s to minutes	10 ppbv	~ 1%	Flight demonstrated during ABLE-3A	
	IR rare gas laser absorption	Continuous or direct	.05 s to minutes	10 ppbv	To be evaluated	Under development. Field tested during ABLE-3A	Kolb et al., 1986 McManus et al., 1988
	Gas-filter-correlation IR absorption, with sampling	Continuous	1 s	10 ppbv	Negligible drift over a normal 15-min. sampling period	Minimum detectable flux of 3×10^{-11} kg CH_4 m^{-2} s^{-1} over a 15-min. sampling period	Sebacher and Harriss, 1982; Harriss et al., 1985
	Gas chromatography with flame ionization detector	Batch	Seconds to minutes	10 ppbv	Not applicable	Detector is linear over wide range of concentrations	Steele et al., 1987
NMHC	Gas chromatography with flame ionization detector	Batch	Seconds to minutes	50 pptv	Not applicable	Samples may require concentration before analysis	Sexton and Westberg, 1979; Roberts et al., 1983; Singh et al., 1985

continued

Table 3.2 (Page 2)

Species	Technique	Sampling Method	Sampling Time (Range)	Detection Limit	Stability	Comments	References
Organic acids	Condensation sampling	Batch	> 10 min.	10 pptv	Not applicable		Dawson and Farmer, 1988
	Mist chamber	Batch	30 min.	Not known	Not applicable		Cofer et al., 1985; Cofer and Edahl, 1986; Andreae et al., 1988a
	Denuder tubes	Batch	60 min.	Not known	Not applicable		Norton, 1986
	Impregnated filters	Batch	60 min.	Not known	Not applicable	Known interferences	Keene et al., 1989
Carbonyls	2, 4-DNPH impregnated cartridge followed by HPLC	Batch	120 min.	Not known	Not applicable		Kunts et al., 1980; Grosjean and Fung, 1982
	Condensation sampling followed by gas chromatography with flame ionization detector	Batch	60–120 min.	1–10 pptv	Not applicable		Snider and Dawson 1985

Table 3.3 Current Species Measurement Technologies — Sulfur Chemical Species

Species	Technique	Sample Method	Sampling Time (Range)	Detection Limit	Stability	Comments	References
Total sulfur	Flame photemetric detection	Continuous sampled or batch	~ 0.5 sec. ~ 10 min.	0.5 ppb @ 0.02 ℓ/min (~ 2 pg S s^{-1}) 3 pg S/sample 2 pptv/1 ℓ sample	1–2% ~ 1%	SF_6 doped FPD. Careful flow control required on all flows. Sensitivity is species dependent. Hydrocarbon interferences	D'Ottavio et al, 1981
	Conversion to SF_6/electron capture detection	Continuous sampled or batch	~ 0.5 sec. ~ 10 min.	~ 50 pptv @ 20 cm^3/min. ~ 0.2 pg S s^{-1} ~ .03 pg S/sample	? ?	Estimates from GC application below. Conversion to SF_6 followed by F_2 removal by catalysis	New technique See GC application below
	Metal foil collection/flash vaporization/flame photometric detection	Batch	~ 10 min.	~ 20 pg S/sample	?	Collects predominantly reduced sulfur. Non-speciated flash vaporization from arbitrarily large sample. Some H_2O interference	Kagel and Farwell, 1986

continued

Table 3.3 (Page 2)

Species	Technique	Sample Method	Sampling Time (Range)	Detection Limit	Stability	Comments	References
SO_2	UV-fluorescence	Continuous sampled	1 min. and up	~ 3 ppbv	~ 30%	Elimination of H_2O interference requires teflon cell	Schwarz et al., 1974
	Chemiluminescence	Batch	> 10 min.	~ 4 ng S/batch ~ 3 ppb/ 1ℓ sample	~ 2%	Impregnated filters, wet chemical handling, capable of large samples	Meixner & Jaeschke 1984
	Laser-induced fluorescence	Direct, no sampling	3-5 s	200 pptv	~ 10%	Near maximum achievable sensitivity	Bradshaw et al, 1985
	Vacuum UV flash photolysis/ laser-induced fluorescence	Direct, no sampling	0.1–2000 s	150 pptv	10–20%	Under development	Bradshaw et al., 1988
	Differential UV absorption	Continuous	>1.0 s	~ 20 ppbv		Has been used for eddy-correlation measurements in very polluted regions (H. Nestler, Heidelberg U.). Sensitivity of 0.01 ppbv for sampling sensitivity times of ~ 20 min.	Platt and Perner, 1980
	Tunable diode laser	Direct, no sampling or continuous	0.1-100 s	~ 1 ppbv (closed cell) ~ ppbv (open cell)	1%	Under development; may be improved by a factor of 20 with astimatic off-axis resonator	Edwards & Ogram, 1986; Hastie et al., 1983; Kolb et al., 1986
$SO_4^=$	Ion chromatography	Batch	> 10 min.	~ 5 pptv	Not applicable	Requires a large sample. Requires column separation	Andreae et al., 1987

continued

Table 3.3 (Page 3)

Species	Technique	Sample Method	Sampling Time (Range)	Detection Limit	Stability	Comments	References
Dimethyl-sulfide	Gas chromato-graphy flame photometric detection	Batch	~ 10 min.	3 pg S/sample ~ pptv/ 1 ℓ sample	~ 1%	Requires GC separation SF_6 doped FPD. Very important O_3 interference	Goldan et al., 1987 Andreae et al., 1985
	Chemilumines-cent detection	Contin-uous sampled or batch	~ 1 s 10 min.	~ 200 pptv ~ pptv/ 1 ℓ sample	?	Interferences from other reduced sulfur compounds or requires GC separation. New technique. Little experience	Nelson et al., 1983
	Gold wool collection/thermal desorption/flame photometric detection	Batch	~ 10 min.	20 pg S/sample	~ 2%	Requires CG separation. Large O_3 interference	Bernard, 1982
	Conversion to SF_6 electron capture detection	Batch	~ 10 min.	~ 0.03 pg S/sample	?	Requires GC separation conversion to SF_6 with F_2 catalytic removal of excess F_2. New technique	Johnson and Lovelock, 1988
H_2S	Gas chromato-graphy flame photo-metric detection	(Same as for dimethyl sulfide using same technique as described above.)			GC separation	No significant O_3 interference. Requires	
	Conversion to SF_6 electron capture detection	(Same as for dimethyl sulfide using same technique as described above)				Requires GC separation	

continued

Table 3.3 (Page 4)

Species	Technique	Sample Method	Sampling Time (Range)	Detection Limit	Stability	Comments	References
	Filter collection FMA fluorescence quenching	Batch	10–60 min.	~ 3 ng S/sample	~50% @ 5 ppt	Large filter-to-filter background variability	Natusch et al., 1972
	Gold collection/ flame photometric detection	Batch	10–100 min.	10 pg S/sample	?	Large chance for variability of H_2S collection efficiency. Requires SO_2 removal. Interference from other reduced sulfur compounds	Braman et al., 1978
OCS	Gas chromatography flame photometric detection	(Same as for dimethyl sulfide using same technique as described above)				No O_3 interference. Requires GC separation	
	Conversion to SF_6 electron capture detection	(Same as for dimethyl sulfide using same technique as described above)				Requires GC separation	
CS_2	Gas chromatography Flame photometric detection	(Same as for dimethyl sulfide using same technique as described above)				Requires GC separation. Small O_3 interference	
	Conversion to SF_6 electron capture detection	(Same as for dimethyl sulfide using same technique as described above)				Requires GC separation	

continued

Table 3.3 (Page 5)

Species	Technique	Sample Method	Sampling Time (Range)	Detection Limit	Stability	Comments	References
	Vacuum UV flash photolysis/ laser-induced fluorescence	Direct, no sampling	0.1-2000 s	150 pptv	10-15%	Under development	Rodgers et al., 1986
CH_3SH	Gas chromatography/flame photometric detection	(Same as dimethylsulfide but less ozone interference)					
Methane sulfonic acid	Ion chromatography	(Similar to $SO_4^=$ aerosols as listed above)					
Dimethyl sulfoxide and dimethyl sulfonic acid	Gas chromatography/flame photometric detection	Batch	2–30 min.	Similar to dimethyl sulfide	~ 1%	Requires silica gel preconcentration	Harvey and Lang, 1986

Table 3.4

Concentration Techniques for Sulfur Species

Species	Technique	Recovery	References
H_2S	Impregnated filter	Liquid extraction	Natusch et al., 1972 Jaeschke & Herman, 1981
SO_2	Impregnated filter	Liquid extraction	Meixner & Jaeschke, 1984 Ockelmann & Georgii, 1984
Reduced sulfur compounds	Palladium foil	Flash evaporation	Kagel & Farwell, 1986
Reduced sulfur compounds	Gold or wool	Nondestructive thermal desorption	Barnard et al., 1982 Ammons, 1980
COS, CS_2	Tenax GC	Nondestructive thermal desorption	Steudler & Kijowski, 1984
All	Glass, bead bed/ cryogenic enrichment	Nondestructive thermal desorption	Farwell et al., 1979 Farwell & Gluck, 1980
All	Open tubular/ cryogenic enrichment	Nondestructive thermal desorption	Goldan et al., 1987

Aerosol Detectors

Aerosols are involved in the atmospheric cycles of several trace gases with important consequences on rates of deposition, as well as potential climatic effects. Many trace species have solid phases in the atmosphere (e.g., $SO_4^=$), with straightforward consequences. In other cases (e.g., chemical composition changes associated with aging sea salt aerosol), the involvement is more complex. For some, such as mineral and organic particles suspended and transported by the wind, the interactions may be more subtle. There is a need to define the surface emission fluxes of primary aerosols, surface deposition of both primary and secondary aerosols, and the flux divergence due to gas-to-particle conversion.

The definition of aerosol fluxes is intrinsically more complex than that for gases, as the definition must generally include information on both the size distribution and composition of the aerosols. In recent years, fast, high-resolution particle detectors have been developed. The most commonly used is a laser-optical particle counter. Electric charge devices have also been used for covariance measurements (Wesely et al., 1977). Flame photometric devices are capable of accurate measurement of some elements contained in aerosols (e.g., S and Na). These devices are generally fast and accurate enough for flux measurements (Hicks et al., 1988).

Additional intricacy arises when the aerosol size distribution is itself modified by the mean humidity profile, or when the aerosol fall velocity approaches the friction velocity. Fairall (1984) has addressed the effects of the humidity profile, as well as other aerosol flux measurement techniques. Lenschow and Kristensen (1985) have addressed the effects of a finite number of particles in estimating a particle flux.

The critical questions requiring aerosol flux measurements to address the role of aerosols in the atmospheric cycles of trace species and their potential for climate change are:

- What is the deposition efficiency of different vegetated surfaces as a function of atmospheric and plant conditions?
- What is the potential for wind-generated emission flux for different areas of the earth's surface as a function of seasonal and climate conditions? What is the potential for long-range transport of these particles?
- What are the emission and deposition fluxes of sea salt under various weather conditions, and what sort of chemical fractionation can occur within the sea salt aerosol due to gas-particle interactions?

We strongly recommend that any ocean-atmosphere flux experiment include a particle flux component.